THEORETICAL STUDY OF THE $NN \to NN\pi\pi$ REACTION

L. Alvarez-Ruso[1], E. Oset[1] and E. Hernández[2],

[1] *Departamento de Física Teórica and IFIC, Centro Mixto Universidad de Valencia - CSIC, 46100 Burjassot (Valencia) Spain.*

[2] *Departamento de Física, Universidad de Salamanca, Spain.*

Abstract

We have developed a model for the $NN \to NN\pi\pi$ reaction and evaluated cross sections for the different charged channels. The low energy part of those channels where the pions can be in an isospin zero state is dominated by N^* excitation, driven by an isoscalar source recently found experimentally, followed by the decay $N^* \to N(\pi\pi)^{T=0}_{S-wave}$. At higher energies, and in channels where the pions are not in T=0, Δ excitation mechanisms become relevant. A rough agreement with the experimental data is obtained in most channels. Repercussions of the present findings for the ABC effect and the $pp \to pp\pi^0$ reaction close to threshold are also suggested.

PACS numbers : 13.75.Gx, 14.20.Gk, 25.75.Dw
Keywords : Two pion production, resonance excitation, N^* decay

1 Introduction

Pion production in NN collisions is one of the sources of information on the NN interaction and about nucleon resonance properties. Particularly the two pion production channel might be especially enlightening in view of the interesting information obtained from the study of analogous reactions with two pions in the final state, the $\pi N \to \pi\pi N$ and $\gamma N \to \pi\pi N$ reactions.

The $\pi N \to \pi\pi N$ reaction close to threshold has been a testing ground for chiral symmetry [1] in the πN sector, although as one goes away from threshold the contribution of resonances becomes important [2]. Even at threshold there is an important non-vanishing contribution from N^* (1440) excitation followed by the decay $N^* \to N(\pi\pi)^{T=0}_{S-wave}$ [2]. With the formalisation of chiral perturbation theory one can further exploit the ideas of chiral symmetry and perform calculations including loops with effective Lagrangians [3]. The Roper resonance still plays and important role but one can use effective Lagrangians involving resonances up to order $O(p^2)$, which generalise the coupling of the $N^* \to N(\pi\pi)^{T=0}_{S-wave}$ transition used in Ref. [2] and introduce one new degree of freedom into the scheme [3].

In the $\gamma N \to \pi\pi N$ reaction, which has also been the subject of study at threshold as a further test of chiral symmetry [4, 5], one of the most interesting results is the role of the $N^*(1520, J^\pi = 3/2^-)$ resonance [6]. The mechanism of N^* (1520) photoexcitation followed by the decay into $\Delta\pi$ interferes with the dominant Kroll Ruderman $\Delta N\pi\gamma$ term and allows one to obtain information about the N^* (1520) $\to \Delta\pi$ decay amplitudes, additional to the one obtained from the analysis of the $\pi N \to \pi\pi N$ reaction [7], and which poses new challenges to quark models of baryons [8]. Roper excitation also plays an important role at threshold in the $\gamma N \to \pi\pi N$ reaction but its role is shadowed by the contribution of other resonances at higher energy [9].

A common feature of the $\pi N \to \pi\pi N$ and $\gamma N \to \pi\pi N$ reactions at threshold is the role of the N^* (1440) followed by its decay into $N(\pi\pi)^{T=0}_{S-wave}$. This gives us a hint that Roper excitation might also play an important role in the $NN \to NN\pi\pi$ reaction close to threshold. On the other hand, contrary to the case of N^* excitation from πN and γN, which is well known, now we have to deal with the $NN \to NN^*$ transition which is not so well explored as the one baryon vertices. An important step in understanding the $NN \to NN^*$ reaction was given with the experiment of Ref. [10] which showed a relatively large strength for N^* excitation due to the exchange of an isoscalar source, the only one allowed in the (α, α') reaction on the proton when this proton is excited to the Roper. The experiment has been analysed in Ref. [11], where the large background from delta excitation in the projectile and an important interference term between the latter mechanism and the one from Roper excitation in the target are properly accounted for. The analysis provides the strength for the isoscalar $NN \to NN^*$ transition which turns out to be large compared to ordinary one pion exchange.

The combination of this N^* isoscalar excitation with the $N^* \to N(\pi\pi)^{T=0}_{S-wave}$ decay seems then called to play an important role in the $NN \to NN\pi\pi$ reaction and this will be the case, as we shall see. On the other hand in the $NN \to NN\pi\pi$ reaction there are many terms which contribute, starting from the set of terms provided by

chiral Lagrangians, plus terms mediated by Δ resonance excitation. We study all these terms asserting their relevance as a function of energy. Furthermore we observe that the weight of the different terms varies appreciably from channel to channel and hence the combined information from these channels puts strong tests to the model.

The comparison with the limited experimental information available on this reaction [12, 13, 14] shows that a rough agreement in most channels can be obtained. Remaining discrepancies in some channels are discussed.

2 Contribution from non-resonant terms

The model that we use is depicted diagrammatically in Fig. 1 and contains terms proceeding through baryon resonance excitation and other non-resonant terms. The latter ones are shown in diagrams (1), (2), (3) and require the knowledge of the $\pi N \to \pi N$ amplitude, the πNN vertex, the $\pi\pi \to \pi\pi$ amplitude and the $NN\pi\pi\pi$ vertex. In the spirit of the phenomenological approach followed here, we take the empirical $\pi N \to \pi N$ amplitude. The other ingredients are derived from the lowest order SU(2) chiral Lagrangians at tree level [15, 16].

The lowest chiral Lagrangians which we need are given by

$$\mathcal{L} = \mathcal{L}_2 + \mathcal{L}_1^{(B)} \tag{1}$$

where $\mathcal{L}_2$ is the Lagrangian in the meson sector and $\mathcal{L}_1^{(B)}$ contains the baryon sector with the meson baryon interactions. We have

$$\mathcal{L}_2 = \frac{f^2}{4} < \partial_\mu U^\dagger \partial^\mu U + M(U + U^\dagger) > \tag{2}$$

$$\mathcal{L}_1^{(B)} = \bar{\Psi}(i\gamma^\mu \nabla_\mu - M_B + \frac{g_A}{2}\gamma^\mu\gamma_5 u_\mu)\Psi\,, \tag{3}$$

where the symbol $<>$ denotes the flavour trace of the $SU(2)$ matrices and U, u are 2×2 matrices

$$U(\phi) = u(\phi)^2 = exp\,(i\sqrt{2}\Phi/f) \tag{4}$$

where

$$\begin{aligned} \Phi(x) &\equiv \tfrac{1}{\sqrt{2}}\,\vec{\tau}\,\vec{\phi} \\ &= \begin{pmatrix} \frac{1}{\sqrt{2}}\pi^0 & \pi^+ \\ \pi^- & -\frac{1}{\sqrt{2}}\pi^0 \end{pmatrix} \end{aligned} \tag{5}$$

and

$$\Psi = \begin{pmatrix} p \\ n \end{pmatrix}. \tag{6}$$

The mass matrix M appearing in Eq. (2), in the limit of $m_u = m_d$, is

$$M = \begin{pmatrix} m_\pi^2 & 0 \\ 0 & m_\pi^2 \end{pmatrix} . \tag{7}$$

Furthermore, ∇_μ is a covariant derivative defined as

$$\begin{aligned} \nabla_\mu \Psi &= \partial_\mu \Psi + \Gamma_\mu \Psi \, , \\ \Gamma_\mu &= \tfrac{1}{2}(u^\dagger \partial_\mu u + u \partial_\mu u^\dagger) \, , \\ u_\mu &= i u^\dagger \partial_\mu U u^\dagger \, . \end{aligned} \tag{8}$$

By expanding the Lagrangian $\mathcal{L}_2$ up to order $O(\phi^4)$ and keeping the interaction terms in $\mathcal{L}_1^{(B)}$ up to order $O(\phi^3)$ as done in Ref. [17], we obtain the diagrams (1), (2) and (3) of Fig. 1 which contribute to the $NN \to NN\pi\pi$ reaction.

The term with $\Gamma_\mu \Psi$ in $\mathcal{L}_1^{(B)}$ contributes to the isovector part of the s-wave πN amplitude. The isoscalar part of this amplitude is zero at this order in the chiral expansion and empirically is much smaller than the isovector one. The isoscalar amplitude is generated when terms of order $O(p^2)$ in the baryon chiral Lagrangian are introduced [3]. In this latter reference the couplings of the new Lagrangians are deduced from empirical information of the πN amplitude in Ref. [3]. With the same philosophy we take the isoscalar πN amplitude from experiment and add it to the vector part. It is customary to write the isoscalar $\pi N \to \pi N$ amplitude in terms of λ_1. Using Mandl and Shaw normalisation [18] ($-it \equiv \mathcal{M}$ of Mandl and Shaw) one has

$$-it^{(s)} = -i4\pi \frac{2\lambda_1}{\mu} \quad ; \quad \lambda_1 = 0.0075 \quad ; \quad \mu \equiv m_\pi \tag{9}$$

which is diagonal in spin and isospin. The isovector part for $p\pi^+ \to p\pi^+$ amplitude is given by

$$-it^{(v)} = -i\frac{1}{4f^2} \bar{p} \gamma^\mu p (p_\mu + p'_\mu) \tag{10}$$

where p, p' are the initial, final pion four-momenta and $\bar{p}$ (p) besides the γ^μ matrix stand for the spinor of the final (initial) protons. This would compare with the usual empirical form of the low energy amplitude

$$-it^{(v)} = -i4\pi \frac{\lambda_2}{\mu^2} (p + p')^0 \tag{11}$$

which comes from Eq. (10) by retaining the dominant zero component, with the equivalence $\lambda_2 = \mu^2/16\pi f^2$, which holds up to 15%. We divert from the standard chiral expansion and use the empirical πN amplitudes in our evaluations.

Eq. (10) is trivially modified in the other isospin channels: same factor in $n\pi^- \to n\pi^-$, relative minus sign in $\pi^+ n \to \pi^+ n$ and $\pi^- p \to \pi^- p$, zero contribution for $\pi^0 p(n) \to \pi^0 p(n)$, extra factor $\sqrt{2}$ for $\pi^- p \to \pi^0 n$ and $\pi^0 n \to \pi^- p$ and extra factor $-\sqrt{2}$ in $\pi^0 p \to \pi^+ n$ and $\pi^+ n \to \pi^0 p$.

The amplitudes $\pi\pi \to \pi\pi$ come from the expansion of $\mathcal{L}_2$ up to order $O(\phi^4)$. In the diagram (1) of Fig. 1 they appear with two pions off shell. We need four charged

amplitudes from where we deduce the rest by using crossing symmetry. We shall give the explicit expressions only in the $\pi^0\pi^0 \to \pi^+\pi^-$ reaction. The expressions for the other channels can be obtained in a similar way. We get

$$-it = i\frac{1}{3f^2}(3m_\pi^2 + 4p^+ \cdot p^- + 2q \cdot q') \tag{12}$$

where q, q' are the π^0 momenta and p^+, p^- the momenta of π^+ and π^- respectively.

The other vertex needed is the πNN which comes from the g_A terms of Eq. (3) expanding up to $O(\phi)$. For $\pi^0 pp$ and an outgoing π^0 with momentum q it is given by

$$-it = \frac{g_A}{2}\frac{1}{f}\,\bar{p}\gamma^\mu\gamma_5 p q_\mu \tag{13}$$

which in the non-relativistic description is $-\frac{f_{\pi NN}}{\mu}\vec{\sigma}\vec{q}$, the standard Yukawa coupling, with the equivalence $g_A/2f = f_{\pi NN}/\mu$.

Finally the other ingredient needed is the three pion vertex which comes from the expansion of the g_A term in Eq. (3) up to order $O(\phi^3)$. For $\pi^0 p \to p\pi^+\pi^-$, with q' the π^0 momentum we obtain

$$-it = \frac{g_A}{2}\bar{p}\gamma^\mu\gamma_5 p\frac{1}{12f^3}(2p_\mu^+ + 2p_\mu^- + 4q'_\mu) \tag{14}$$

and similar expressions in other isospin channels.

With these ingredients one constructs immediately the contribution from diagrams (1)-(3) of Fig. 1 for the $pp \to pp\pi^+\pi^-$ case by following the standard Feynman rules. As an example, the term corresponding to the diagram (1) of Fig. 1 for $pp \to pp\pi^+\pi^-$ is given by

$$\begin{aligned} -it = \;& i\tfrac{1}{3f^2}(3m_\pi^2 + 4p^+ \cdot p^- + 2q \cdot q')\,. \\ & \tfrac{1}{q^2-m_\pi^2}\tfrac{1}{q'^2-m_\pi^2}(\tfrac{g_A}{2}\tfrac{1}{f})^2\,(\bar{p}\gamma^\mu\gamma_5 p q_\mu)_1\,(\bar{p}\gamma^\nu\gamma_5 p q'_\nu)_2 \end{aligned} \tag{15}$$

where the indices 1 and 2 refer to the first and second nucleons respectively. In the Appendix we further reduce this expression to a Pauli spinor notation and care explicitly about baryon antisymmetry, the symmetry of the diagrams and off shell form factors.

3 Δ resonance terms contribution

Next we introduce terms with Δ excitation. We need the $\pi N\Delta$ coupling, whose vertex is given in a Pauli spinor notation by

$$-i\delta\tilde{H}_{\pi N\Delta} = \frac{f^*}{\mu}\vec{S}^\dagger\vec{q}\,T^{\dagger\lambda} \quad + \quad h.c. \tag{16}$$

corresponding to the vertex $\pi^\lambda + N \to \Delta$, with λ the isospin index of the pion, q its momentum and $\vec{S}^\dagger$ ($\vec{T}^\dagger$) the spin (isospin) transition operators from 1/2 to 3/2 with the normalisation

$$\left\langle \frac{3}{2}, M \right| S_\nu^\dagger \left| \frac{1}{2}, m \right\rangle = C\left(\frac{1}{2}, 1, \frac{3}{2}; m, \nu, M\right) \tag{17}$$

where ν is the spherical component of $\vec{S}^\dagger$ and same normalisation for $\vec{T}^\dagger$.

We shall also need the $\pi\Delta\Delta$ vertex for $\pi\Delta \to \Delta$ given by

$$-i\delta\tilde{H}_{\pi\Delta\Delta} = \frac{f_\Delta}{\mu}\vec{S}_\Delta \vec{q}\, T_\Delta^\lambda \tag{18}$$

where now $\vec{S}_\Delta$ ($\vec{T}_\Delta$) are the ordinary spin (isospin) matrices for spin (isospin) 3/2. Two properties involving sums over intermediate Δ spins are needed in the evaluation of the diagrams and they are

$$\sum_M S_i \left|M_s\right\rangle \left\langle M\right| S_j^\dagger = \frac{2}{3}\delta_{ij} - \frac{i}{3}\epsilon_{ijk}\sigma_k \tag{19}$$

$$\sum_{M,M'} S_i \left|M'\right\rangle \left\langle M'\right| S_{\Delta,j} \left|M\right\rangle \left\langle M\right| S_k^\dagger = \frac{5}{6}i\epsilon_{ijk} - \frac{1}{6}\delta_{ij}\sigma_k + \frac{2}{3}\delta_{ik}\sigma_j - \frac{1}{6}\delta_{jk}\sigma_i \tag{20}$$

For the coupling constants we take, $f^{*2}/4\pi = 0.36, \quad f_\Delta/f_{\pi NN} = \frac{4}{5}$, where the first one is empirical and the second one comes from the quark model. The couplings in Eq. (16) (18) have to be evaluated in the rest frame of the created Δ.

With these new ingredients and those of the former section one can evaluate the diagrams (9)-(15) which appear in Fig. 1. The expressions for the amplitudes of the relevant terms are written in the Appendix. As we shall see, all these terms are small except diagram (12), the one involving the excitation of a Δ in each nucleon. This diagram is only relevant at energies $T_p > 1\ GeV$ in the laboratory frame, where the terms involving crossed Δ are small (diagrams (13)-(15)). At lower energies all of them become negligible since they involve two p-wave couplings of the pions (diagrams (10) and (11) involve only one p-wave coupling but they are small anyway since the s-wave coupling is comparatively small).

One warning is however in order with respect to diagrams (9), (12)-(15) in Fig. 1 which involve two p-wave couplings. When this is the case one must take into account the indirect effect of the rest of the NN interaction, particularly the repulsive force at short distances. This is so because the combination of the pion propagator and the p-wave couplings contains a $\delta(\vec{r})$ force which becomes inoperative in the presence of short range correlations. We follow a standard procedure to account for this which is to substitute

$$\hat{q}_i\hat{q}_j D(q) \to V_L'(q)\,\hat{q}_i\hat{q}_j + V_T'(q)(\delta_{ij} - \hat{q}_i\hat{q}_j) \tag{21}$$

which substitutes the pure spin longitudinal pion exchange by a mixture of spin longitudinal and transverse contributions. Following Ref. [19] we take

$$
\begin{aligned}
V'_L(q) &= V'_\pi(q) + g'_l(q)\,, \\
V'_T(q) &= V'_\rho(q) + g'_t(q)\,, \\
V'_\pi(q) &= F^2_\pi(q^2)\vec{q}^{\,2} D_\pi(q)\,, \\
V'_\rho(q) &= F^2_\rho(q^2)\vec{q}^{\,2} D_\rho(q) C_\rho\,, \\
g'_l(q) &= -(\vec{q}^{\,2} + \tfrac{1}{3}q_c^2)\tilde{F}^{\,2}_\pi \tilde{D}_\pi{}^2 - \tfrac{2}{3}q_c^2 \tilde{F}_\rho{}^2 \tilde{D}_\rho C_\rho\,, \\
g'_t(q) &= -\tfrac{1}{3}q_c^2 \tilde{F}_\pi{}^2 \tilde{D}_\pi - (\vec{q}^{\,2} + \tfrac{2}{3}q_c^2)\tilde{F}_\rho{}^2 \tilde{D}_\rho C_\rho
\end{aligned}
\tag{22}
$$

where $D_{\pi,\rho}(q)$ are the meson propagators and $F_{\pi,\rho}(q)$ are meson form factors of the monopole type with $\Lambda_\pi = 1.3\ GeV$, $\Lambda_\rho = 1.4\ GeV$ and $C_\rho = 3.94$, consistent with the Bonn model [20]. The corresponding functions with a tilde are obtained by substituting, in the argument q of the function, $\vec{q}^{\,2}$ by $\vec{q}^{\,2} + q_c^2$, where $q_c = 780\ MeV$, the inverse of the short range correlations scale.

4 $N^*(1440)$ terms contribution

Next we introduce the $N^*\,(1440)$ excitation. The N^* couples to $N\pi\,, \Delta\pi\,, N(\pi\pi)^{T=0}_{S-wave}$ as important decay channels. The corresponding vertices are given by

$$
-\,i\delta\tilde{H}_{\pi N N^*} = \frac{\tilde{f}}{\mu}\vec{\sigma}\vec{q}\tau^\lambda \;+\; h.c. \tag{23}
$$

$$
-\,i\delta\tilde{H}_{\pi N^*\Delta} = \frac{g_{\pi N^*\Delta}}{\mu}\vec{S}^{\,\dagger}\vec{q}\,T^\lambda \tag{24}
$$

both evaluated in the N^* rest frame. The coupling constants are $\tilde{f} = 0.477$ and $g_{\pi N^*\Delta} = 2.07$ [8].

For the $N^* \to N(\pi\pi)^{T=0}_{S-wave}$ decay channel, which accounts for $5-10\%$ of the total width according to the particle data table [21], we take the $O(p^2)$ Lagrangian as given in Ref. [3] using an SU(2) formalism

$$
\mathcal{L}_{N^*N\pi\pi} = c_1^*\bar{\psi}_{N^*}\chi_+\psi_N - \frac{c_2^*}{M^{*\,2}}(\partial_\mu\partial_\nu\bar{\psi}_{N^*})u^\mu u^\nu\psi_N + h.c. \tag{25}
$$

where

$$
\chi_+ = \mu^2(2 - \frac{\vec{\phi}^{\,2}}{f^2} + \ldots)\,;\; u_\mu = -\frac{1}{f}\vec{\tau}\partial_\mu\vec{\phi} + \ldots \tag{26}
$$

and $\vec{\phi}$ stands for the pion field. Hence, expanding up to second order in the pion fields and keeping the largest $\mu,\nu = 0,0$ components, which neglects terms of order $O(\frac{p^2}{M^{*2}})$, we find

$$
\mathcal{L}_{N^*N\pi\pi} = -c_1^*\mu^2\bar{\psi}_N\frac{\vec{\phi}^{\,2}}{f^2}\psi_N + c_2^*\bar{\psi}_{N^*}\frac{1}{f^2}(\vec{\tau}\partial_0\vec{\phi})(\vec{\tau}\partial_0\vec{\phi})\psi_N + h.c. \tag{27}
$$

This Lagrangian leads to an effective vertex

$$-i\delta\tilde{H}_{N^*N\pi\pi} = -i\,2\,\frac{\mu^2}{f^2}\left(c_1^* + c_2^*\frac{\omega_1\omega_2}{\mu^2}\right) \tag{28}$$

for $\pi^+\pi^-$ and $\pi^0\pi^0$ creation and zero otherwise. Here ω_1, ω_2 are the energies of the pions.

Following the steps of Ref. [3] we fit the experimental width from $\pi^0\pi^0$ plus $\pi^+\pi^-$ final states

$$\Gamma_{N^*\pi\pi} = \alpha(c_1^*)^2 + \beta(c_2^*)^2 + \gamma c_1^* c_2^* \tag{29}$$

and we take $\Gamma_{N^*N\pi\pi}$ assuming $\Gamma^*_{N^*\,tot} = 350\,MeV$ [21] and branching ratio of 7.5% for the $N(\pi\pi)^{T=0}_{S-wave}$ decay channel. We obtain $\alpha = 0.497\,10^{-3}\,GeV^3$, $\beta = 3.66\,10^{-3}\,GeV^3$ and $\gamma = 2.69\,10^{-3}\,GeV^3$. These values are somewhat different from those of Ref. [3] where a smaller width for the Roper was taken. With the c_1^* parameter alone one gets a solution for that parameter, but with the two parameters one gets an ellipse in c_1^*, c_2^*. This ellipse spans over a large range of values of c_1^*, c_2^*. It is clear that one needs further constrains in order to determine c_1^* and c_2^*. We use the $\pi^- p \to \pi^+\pi^- n$ reaction in order to impose such constrains. For this purpose we use the model of Ref. [2]. The cross section shows a strong sensitivity to the values of c_1^*, c_2^* and spans about two orders of magnitude when the values of these parameters are varied along the ellipse of Eq. (29) (details can be seen in Ref. [22]). The best agreement with the experiment is obtained with $c_2^* = 0$, which corresponds to $c_1^* = -7.27\,GeV^{-1}$ (set I). However, the experimental errors are compatible with the use of $c_1^* = -12.7\,GeV^{-1}$, $c_2^* = 1.98\,GeV^{-1}$ (set II) and intermediate values in the ellipse. In order to illustrate the uncertainties in c_1^*, c_2^* we plot the cross sections using the extreme values of these parameters, compatible with the $\pi^- p \to \pi^+\pi^- n$ cross sections, quoted above. A best fit to the different $\pi N \to \pi\pi N$ channels is done in [23] using a Lagrangian for the $N^* \to N(\pi\pi)^{T=0}_{S-wave}$ process, equivalent to the one of Eq. (27) at low energies. Although the data would roughly be compatible with the use of $c_2^* = 0$, they obtain a best fit with other set of parameters. However, this work contains some small differences with respect to the model of Ref. [2], like the relativistic treatment, the use of an N^* width assuming phase space for πN decay only and the neglect of the isoscalar πN amplitude and intermediate $\Delta\Delta$ states (which are included in [2]). These are small differences, but they have some influence in the c_1^* and c_2^* parameters. For the reason of consistency with our input, we take the values of c_1^* and c_2^* from our own analysis.

The diagrams which we obtain now with these new ingredients are (4)-(8) of Fig. 1. Diagrams (4) and (5) are relevant but (6) and (7) give a much smaller contribution. Diagram (8) is also important because both N^* and Δ can be placed simultaneously on shell. Note that we disregard terms like (8) or (9) with crossed N^* or Δ poles. Also in the case of the N^* we disregard the term with two N^* excitations, both in the same nucleon or in different ones. Because the πNN coupling is about one fourth of the $\pi N\Delta$ one, and the N^* propagator would be placed on shell at higher energies, these terms are small compared to the corresponding ones with two Δ or $N^*\Delta$ excitation in the energy range where we are.

In Fig 1. we have explicitly shown what kind of particle exchange we consider. For instance, in diagrams (6), (7) we exchange one of the pions coming from the N^* decay. In diagrams (4), (5) and (8) we consider the effective isospin T=1 interaction of Eq. (21), but in addition we must consider an exchange in the T=0 channel, to which we come below.

The analysis of the (α, α') reaction on a proton target [10] carried out in Ref. [11] interpreted the results in base of two mechanisms: Δ excitation in the projectile depicted in Fig. 2 (a) and N^* (1440) excitation in the proton target, Fig 2 (b). However, an important interference was found between the mechanism of Δ excitation in the projectile and N^* excitation in the target followed by the decay of the N^* into $N\pi$. Since the ^4He beam has $T = 0$ the N^* excitation in the (α, α') reaction requires the exchange of an isoscalar object. In meson exchange pictures it could be σ or ω exchange. However, the experiment has not enough information to provide the separate strength of both ingredients and only the strength of the combined exchange can be extracted. This transition amplitude was parametrised in Ref. [11] in terms of an effective "σ" which couples to NN as the σ exchange of the Bonn model [20] and couples to NN^* with an unknown strength which is determined by a best fit to the data. Hence, we have

$$\begin{aligned} -i\delta\tilde{H}_{\sigma\, NN} = F_\sigma(q) g_{\sigma NN} \quad ; \quad g^2_{\sigma NN}/4\pi = 5.69 \\ -i\delta\tilde{H}_{\sigma\, NN^*} = F_\sigma(q) g_{\sigma NN^*} \end{aligned} \tag{30}$$

where $F_\sigma(q)$ is a form factor of the monopole type with $\Lambda_\sigma = 1700\, MeV$, assumed equal in both vertices. The fit to the data provides a value $g^2_{\sigma NN^*}/4\pi = 1.33$, with $g_{\sigma NN}$ and $g_{\sigma NN^*}$ of the same sign.

In our selection of the relevant diagrams we have excluded those with a nucleon pole. These terms are smaller than those with Δ pole because the πNN coupling is about a factor two smaller than the $\pi N\Delta$ one, and also because there are usually large cancellations between direct and crossed nucleon pole terms. Indeed, assume we have the diagrams (12) and (14) of Fig 1 substituting the left Δ by a nucleon. For small momenta of the outgoing pion, on the left of the diagram we would have for the sum of the two nucleon propagators

$$G^{(a)} + G^{(b)} \simeq \frac{1}{M + m_\pi - M} + \frac{1}{E(\vec{p}\,') - m_\pi - E(\vec{p})} \simeq 0\,. \tag{31}$$

This cancellation would not occur if we had a resonance in the intermediate state since there is a difference of masses and now we would have

$$G^{(a)}_R + G^{(b)}_R \simeq \frac{1}{M + m_\pi - M_R} + \frac{1}{E(\vec{p}) - m_\pi - E_R(\vec{p})} \simeq \frac{1}{m_\pi - \Delta M} + \frac{1}{-m_\pi - \Delta M}\,. \tag{32}$$

We have also omitted terms involving the exchange of vector mesons in diagrams of the type of (1)-(3) in Fig. 1. We estimate their contribution to be small as follows. Take for instance the equivalent of diagram (1) substituting the virtual pions by virtual ρ mesons. A general expression for the $\rho\rho\pi\pi$ Lagrangian is given in [24]. For our purpose

we can get the low energy estimate by using the analogy of the minimal coupling generation of the $\gamma\gamma$ coupling to $\pi\pi$, in which case we obtain a Lagrangian of the type

$$\mathcal{L}_{\rho\rho\pi\pi} = \frac{f_\rho^2}{2}(\vec{\rho}_\mu \cdot \vec{\rho}^\mu)(\vec{\phi} \cdot \vec{\phi}) \tag{33}$$

with $f_\rho = 6.1$, the $\rho\pi\pi$ coupling. The diagram (1) with two virtual ρ mesons is now readily evaluated and we find at the end that its strength is about the same as the corresponding diagram with two virtual pions. Short range correlations also help to further reduce the $\rho\rho$ diagram versus the $\pi\pi$ one. The fact that these meson-meson terms are found to be small altogether suggests that this should also be the case with the inclusion of the ρ meson in the analogous diagrams.

As for the ω exchange, one can think of a diagram like (1) in Fig. 1 substituting one virtual pion by an ω meson. The coupling of the ω to three pions can be found in [24] and is of the type

$$V_{\omega\pi\pi\pi} \propto \epsilon_{\mu\nu\alpha\beta}\epsilon^\mu p_1^\nu p_2^\alpha p_3^\beta \tag{34}$$

where p_i are the momenta of the pions and ϵ^μ the polarisation vector of the ω. We can expect, in principle, contributions similar to the ρ meson case. However, at threshold this term will identically vanish since only the zero components in Eq. (34) will contribute and they are contracted by an antisymmetric tensor. Hence we should expect contributions from this term comparatively smaller than the one from ρ meson exchange discussed above and negligible for the total amplitude.

5 Results and discussion

In the first place let us look at the reaction $pp \to pp\pi^+\pi^-$. We show the cross section as a function of the energy in Fig. 3. We have separated the contribution of several blocks of diagrams in the figure. They are calculated using set I of parameters c_1^*, c_2^*, but the total contribution is given for both sets I and II (solid lines) in order to give an idea of the theoretical uncertainties. Although the sum of the terms is done coherently, there is in fact little interference in the total cross section. The short-dashed curve corresponds to chiral terms, diagrams (1)-(3) of Fig. 1. As we can see, this contribution is negligible in this channel. The dash-dotted curve corresponds to the diagrams (9)-(15) involving only Δ excitations. We see that this contribution is much larger than the former one. At low energies it gives a negligible contribution to the cross section but it rises steeply as a function of the energy and becomes dominant at large energies. Among all these terms, $\Delta\Delta$ excitation mechanism of diagram (12) is the largest above $T_p = 1\ GeV$. The long-dashed curve stands for diagram (8) exciting N^* and Δ consecutively. We can see that this term is more relevant than the set of Δ terms at low energies. Finally we show in the long-short dashed line the contribution of the set of diagrams involving one N^* excitation followed by a two-pion decay in s-wave, diagrams (4)-(7). We can see in the figure that this gives by far the largest contribution at low energies. The sum of all contributions is given by the solid lines. These lines, corresponding to the two acceptable sets of c_1^*, c_2^* parameters, differ by about a factor two at low energies

and about 30 % at $T_p \sim 1\,GeV$. This sets the level of the theoretical uncertainties in this reaction. Another reading of these results is that the $pp \to pp\pi^+\pi^-$ reaction is a more sensitive tool to the $N^* \to N(\pi\pi)^{T=0}_{S-wave}$ couplings than the $\pi N \to \pi\pi N$ reaction and could be used to put stronger constrains on them. In the next section we shall see how these results can be improved. In any case these results have to be seen with the perspective that by omitting the N^* terms the disagreement at energies below $T_p = 900\,MeV$ is larger than two orders of magnitude. The $\Delta\Delta$ mechanism has been used in connection with the ABC effect in the $np \to d + X$ reaction [25], but at energies corresponding to $T_p > 1200\,MeV$ in the elementary reaction. The strength of this term at these energies is sizable but we get two other sources of contribution from N^* excitation, as we have shown, which have about the same strength as the $\Delta\Delta$ term. We should mention, however, that the consideration of short range correlations has decreased the contribution of the $\Delta\Delta$ term with respect to the π exchange alone by about a factor three.

In order to show the relevance of the findings of the isoscalar excitation of the Roper we show in Fig. 4 the contribution of the N^* terms, diagrams (4) and (5) and show there three curves. One with the contribution of the term if we assume a correlated $\pi + \rho$ exchange in the T=1 channel (V'_L, V'_T terms), short-dashed curve, another one with the contribution assuming only "σ" exchange , long-dashed curve, and the third one the results with the sum of the two exchanges, solid line. As we can see, the contribution with "σ" exchange is about one order of magnitude bigger than the one obtained with the correlated $\pi + \rho$ exchange. This shows the importance of the novel findings on the isoscalar Roper excitation in order to understand the 2π production in the pp reaction. This also gives hopes that the permanent problems in the ABC effect, tied to the poor angular dependence provided by the $\Delta\Delta$ model [25, 26] could find a solution in the light of this new interpretation of the $pp \to pp\pi^+\pi^-$ reaction.

In Ref. [27] a different approach was followed based on the one pion exchange model and two mechanisms: one with two pions produced from the same baryon line and another one with a pion produced in each baryon line. The ingredients needed there, the $\pi N \to \pi\pi N$ and $\pi N \to \pi N$ amplitudes, were taken from experimental cross sections, making several assumptions on how to extrapolate them off shell and summing incoherently the contribution of the two mechanisms. The model was used at higher energies that those explored here. Even if phenomenologically one would be considering in [27] the terms discussed here with explicit models, it would only account for the π exchange in the terms with N^* excitation followed by $N \to N(\pi\pi)^{T=0}_{S-wave}$ or $N^* \to \Delta\pi$, while we have shown that the "σ" exchange is the dominant piece in the $NN \to NN^*$ transition. Also, we have seen that the indirect effect of the short range repulsive NN force weakens the π exchange contribution in the 2π production process. Thus, the experience gathered through the years on the NN interaction and the pion nucleon and nuclear interaction, together with the recent findings on isoscalar Roper excitation, have made it possible the detailed model of the present work, clarifying and improving the ideas contained in Ref. [27].

In Fig. 5 we show the results for the $pn \to pn\pi^+\pi^-$ reaction with the same meaning as in Fig. 3 and similar results, although with a larger discrepancy than in the previous case.

In Fig. 6 we show the results off the $pp \to pn\pi^+\pi^0$ channel. This reaction is interesting because the N^* excitation with $N^* \to N(\pi\pi)^{T=0}_{S-wave}$ decay shown in diagrams (4) and (5), which were dominant in the $pp \to pp\pi^+\pi^-$ reaction, do not exist now. Diagrams (6) and (7) still contribute, but they are very small because they involve one $N^*N\pi$ p-wave coupling, which vanishes at threshold and also σ exchange is not allowed. Indeed the $\pi^+\pi^0$ system can only be in $T = 1, 2$ but not in $T = 0$. Hence, the mechanism that was dominant in the $pp \to pp\pi^+\pi^-$ reaction at low energies is not present here. In spite of that, the agreement with the data is of the same quality as the one found before for the $pp \to pp\pi^+\pi^-$ reaction. Now the dominant terms are those exciting Δ's.

In Fig. 7 we show results for the $pn \to pp\pi^-\pi^0$ reaction. The features are qualitatively similar to those in the previous channel but the discrepancies are considerably bigger. We note that the strength of diagram (8) is now comparatively bigger with respect to Δ excitation terms than in the previous case.

In Fig. 8 the results for the $pp \to nn\pi^+\pi^+$ reaction are shown. Here, at high energies, Δ terms are still dominant, but below 1 GeV chiral terms dominate the amplitudes. This is the only case where these terms are relatively important. This also means that we should accept large uncertainties at low energies since, as we saw, there are other terms mediated by ρ meson exchange which are of the same order of magnitude and were neglected here.

In Fig. 9 we show cross sections for the $pp \to nn\pi^0\pi^0$ channel. This is again a channel where the diagrams (4) and (5) are dominant at low energies, like in the $pp \to pp\pi^+\pi^-$ case. Chiral terms are not drawn since they are below the scale of the figure. In this case we overestimate the experimental results by about a factor 2-3 although the quality of the data is not as good as in former cases.

With these results we exhaust the experimental data and the isospin independent channels. Indeed, using the isospin analysis of Ref. [14] one can see that there are only six independent cross sections. For instance one can deduce an interesting relationship with the cross sections which is the following

$$\begin{aligned} 2\sigma(pp\pi^+\pi^-) - \sigma(pn\pi^+\pi^0) - 4\sigma(pp\pi^0\pi^0) + 2\sigma(nn\pi^+\pi^+) \\ +2\sigma(pn\pi^+\pi^-) - 2\sigma(pp\pi^-\pi^0) - 4\sigma(pn\pi^0\pi^0) = 0. \end{aligned} \tag{35}$$

The $NN\pi\pi$ labels stand for the outgoing particles in the given channel. Incoming ones are fixed by charge conservation. We have also calculated the $pn \to pn\pi^0\pi^0$ cross section with our model, as shown in Fig. 10, for which there are no experimental data available. We have checked Eq. (35) independently for the different mechanisms of the model as a test of consistency which has been passed successfully.

The model presented here contains only tree level diagrams. Unitarity is not strictly fulfilled. Actually, imposing unitarity with four particles in the final state is less than trivial, as evidenced by the enormous difficulties in the case of three body final state [28]. However, one should bare in mind that as far as we have dominance of a resonant term, the important aspects of unitarity are included if the proper resonance width is used in the resonance propagator, as we do. Partial unitarization is accomplished by the introduction of loops, as done for instance in the $\pi N \to \pi\pi N$ reaction for the

chiral terms in Ref. [3]. However, we saw that this sector plays a minor role in the present reaction in view of the dominant contribution of resonant terms. Unitarization schemes, as the one of Olsson [29], have proved to be successful in the two body final state when a resonant term is dominant and there is a small background. One multiplies the resonant term by a phase $e^{i\phi}$, with ϕ small in principle, and demand that the resulting amplitude satisfies Watson's theorem, with the global phase of the amplitude in a particular channel equal to the one of the final state. The angles ϕ needed in the problem of $\gamma N \to \pi N$ are of the order of 10° [30]. In order to have a feeling for what could be the effects of imposing unitarity in our model, we took the $pp \to pp\pi^+\pi^-$ channel and multiplied the dominant N^* term by $e^{i\phi}$. We see that for values of ϕ up to 20° the cross section changes at the level of 1%. Rough as the procedure appears to be, it gives hints that unitarity is not a thing to worry much about in the energy domain studied here.

6 Final state interaction

We are going to make a qualitative study of the effect of final state interaction (FSI). Since the energy of the incoming particles is large at $T_p \geq 800\, MeV$, we take plane waves for the initial state and look at modifications only from the interaction of the final particles. Since the low energy region in the $pp \to pp\pi^+\pi^-$ reaction is dominated by the $N^*(\pi\pi)^{T=0}_{S-wave}$ contribution, we concentrate on this mechanism alone in order to assert the effect of the FSI. For this purpose we substitute

$$\tilde{f}(\vec{q}) = F^2(q)\frac{1}{q^{0\,2} - \vec{q}^{\,2} - m_\sigma^2} \tag{36}$$

by

$$\int d^3r \varphi(\vec{r})\, e^{\left(i\,\frac{\vec{p}_1 - \vec{p}_2 + \vec{p}_5 + \vec{p}_6}{2}\,\vec{r}\right)} f(\vec{r}) \tag{37}$$

where $f(\vec{r})$ is the Fourier transform of $\tilde{f}(q)$,

$$f(r) = \int \frac{d^3q}{(2\pi)^3} e^{-i\vec{q}\vec{r}} \tilde{f}(\vec{q}). \tag{38}$$

The momenta are chosen according to Fig. 11. By taking a monopole form factor

$$F(q) = \frac{\Lambda^2 - m_\sigma^2}{\Lambda^2 - q^{02} + \vec{q}^{\,2}} \tag{39}$$

we find

$$\begin{aligned} f(\vec{r}) &= \frac{1}{4\pi}\left\{\frac{\Lambda^2 - m_\sigma^2}{2\tilde{\Lambda}}\, e^{-\tilde{\Lambda}r} + \frac{e^{-\tilde{\Lambda}r}}{r} - \frac{e^{-\tilde{m}_\sigma r}}{r}\right\} \\ \tilde{\Lambda}^{\,2} &= \Lambda^2 - (q^0)^2 \quad ; \quad \tilde{m}_\sigma^2 = m_\sigma^2 - (q^0)^2 \end{aligned} \tag{40}$$

On the other hand $\varphi(\vec{r})$ is the pp final wave function, which for low energies can be written as

$$\varphi(\vec{r}) = e^{\left(i\,\vec{k}\vec{r}\right)} + \tilde{j}_0(k,r) - j_0(kr) \tag{41}$$

where $\vec{k} = (\vec{p}_4 - \vec{p}_3)/2$, $k = |\vec{k}|$ and $\tilde{j}_0(k,r)$ is the interacting pp relative radial wave function with the boundary condition at $r \to \infty$

$$\tilde{j}_0(k,r) \to e^{i\delta_0}\frac{1}{kr}sin(kr+\delta_0) \tag{42}$$

which we calculate with the Paris potential [31]. Thus we finally substitute

$$\begin{aligned} &F^2(q)\tfrac{1}{q^{02}-\vec{q}^2-m_\sigma^2} \to F^2(q)\tfrac{1}{q^{02}-\vec{q}^2-m_\sigma^2} \\ &+4\pi\int_0^\infty r^2\,dr\,j_0(Qr)[\tilde{j}_0(k,r) - j_0(kr))]f(r) \end{aligned} \tag{43}$$

and close to threshold

$$\begin{aligned} &\vec{Q} \simeq \tfrac{\vec{p}_1-\vec{p}_2}{2} = \vec{p}_1 \quad (CM) \\ &q^0 \simeq E(p_1) - M \simeq m_\pi \end{aligned} \tag{44}$$

which simplifies much the computations.

The effect of FSI is an increase of the cross section at low energies with respect to impulse approximation (IA), using plane waves. At high energies, the approximations of Eqs. (43), (44) are not good but one should expect that the IA becomes progressively more accurate. However, one must also take into account that some of the effective couplings are already chosen in a way that they incorporate FSI effects. This is certainly the case in the correlated $\pi + \rho$ exchange which we have discussed. It is also the case in the $NN \to NN^*$ transition dominated by the effective "σ" exchange, since the empirical coupling was obtained in Ref. [11] without explicit inclusion of FSI. Distortions of proton and pion waves in the (α, α') reaction was considered in an eikonal approximation in order to eliminate the α breaking channels. Since the analysis of Ref. [11] was done at an equivalent $T_p \simeq 1\ GeV$, we find an approximate way to account for FSI in the N^* dominated channels in our present calculation by multiplying the cross sections by the factor

$$\frac{\sigma^{FSI}(T_p)}{\sigma^{IA}(T_p)} \cdot \frac{\sigma^{IA}(T_p = 1GeV)}{\sigma^{FSI}(T_p = 1GeV)} \tag{45}$$

up to $T_p = 1\ GeV$ and we do not modify them at energies higher than $T_p = 1\ GeV$. With these considerations we find the results shown in Fig. 12 for the $pp \to pp\pi^+\pi^-$ reaction , which should be taken as indicative of the role played by FSI. We see that the slope of the data is better reproduced when FSI effects are included.

7 Conclusions

We have constructed a model for the $NN \to \pi\pi NN$ reaction consisting of the terms appearing from chiral Lagrangians involving nucleons and pions, plus terms involving the excitation of Δ and N^* (1440). In the channels where the two pions can be in a

$T = 0$ state, as $\pi^+\pi^-$ and $\pi^0\pi^0$, we find a dominance of the N^* excitation in one nucleon decaying into N and $\pi\pi$ in $T = 0$, S-wave. The recent experimental findings about isoscalar N^* excitation in the (α, α') reaction on proton targets are used here and one finds that in the $pp \to pp\pi^+\pi^-$, $pn \to pn\pi^+\pi^-$ reactions the $NN \to NN^*$ transition, driven by the isoscalar "σ" exchange, and followed by the $N^* \to N(\pi\pi)^{T=0}_{S-wave}$ decay largely dominates the cross section at low energies. This is an important finding of the present work which could not have been asserted prior to the experimental observation and analysis of the Roper excitation in the (α, α') reaction. As the energy increases, the N^* excitation followed by $\Delta\pi$ decay takes also a share of the cross section and so does the excitation of a Δ in each of the nucleons, which becomes dominant at energies $T_p > 1300\, MeV$. Other terms which are calculated are found to play a minor role.

A different case is the one of the $pp \to pn\pi^+\pi^0$ channel where the N^* excitation followed by $N^* \to N(\pi\pi)^{T=0}_{S-wave}$ is forbidden. In this case the successive excitation of two Δ on the same nucleon, the Δ excitation on each nucleon, the N^* excitation followed by $\Delta\pi$ decay and even the chiral terms (at low energies) share the strength of the reaction and one obtains a qualitative agreement with experiment. However, these same ingredients used in the $pp \to pp\pi^+\pi^-$ reaction but omitting the $N^* \to N(\pi\pi)^{T=0}_{S-wave}$ decay would give cross sections roughly two orders of magnitude smaller than experiment at low energies. This gives us a qualitative idea of the important role played by this mechanism in this reaction.

These new mechanisms for the $NN \to NN\pi\pi$ reaction are bound to have repercussions in other reactions. The $pp \to pp\pi^0\pi^0$ amplitude with one of the two π^0 produced in one nucleon and absorbed in the other one, gives rise to a box diagram that could be relevant for the $pp \to pp\pi^0$ reaction close to threshold. Similarly, the isotropic piece in $pp \to pp\pi^+\pi^-$ coming from the N^* excitation followed by the 2π decay might be the clue to a better understanding of the ABC effect, which demands such a highly isotropic amplitude in order to interpret the angular dependence [26]. Steps in this direction should be encouraged.

Acknowledgements

We would like to thank useful discussions with M. J. Vicente Vacas. This work is partially supported by CICYT contract number AEN 96-1719. One of us L.A.R. wishes to thank financial support from the Generalitat Valenciana.

Appendix

AMPLITUDES FOR THE $pp \to pp\pi^+\pi^-$ CHANNEL.

In this channel, the total amplitude can be expressed as

$$\mathcal{M}^{(T)} = \mathcal{M}_{r_3r_4r_1r_2}(p_3,p_4,p_1,p_2) - \mathcal{M}(1 \leftrightarrow 2) + \mathcal{M}(3 \leftrightarrow 4, 1 \leftrightarrow 2) - \mathcal{M}(3 \leftrightarrow 4) \quad (46)$$

where the first term in the sum is given below for all mechanisms included in the calculation. The subindex stands for the number of the diagrams in Fig. 1.

$$\begin{aligned}
\mathcal{M}_{1+2} &= i\frac{1}{6f^2}\left(\frac{f_{\pi NN}}{\mu}\right)^2 \left\{ \frac{(\vec{\sigma}\cdot\vec{q_1})_{r_3r_1}(\vec{\sigma}\cdot(3\vec{q_1}+\vec{q_2}))_{r_4r_2}}{q_1^2-\mu^2} \right. \\
&\left. -\frac{(\vec{\sigma}\cdot\vec{q_1})_{r_3r_1}}{q_1^2-\mu^2}\frac{(\vec{\sigma}\cdot\vec{q_2})_{r_4r_2}}{q_2^2-\mu^2}[2(q_1q_2)+4(p_5p_6)+3\mu^2] \right\} F_\pi(q_1)F_\pi(q_2) \qquad (47)
\end{aligned}$$

$$\mathcal{M}_3 = -i(4\pi)^2 \frac{\left\{2\frac{\lambda_1}{\mu} - \frac{\lambda_2}{\mu^2}({q_1}^0 + 2{p_5}^0)\right\}\delta_{r_3r_1}\left\{2\frac{\lambda_1}{\mu} + \frac{\lambda_2}{\mu^2}({q_2}^0 + 2{p_5}^0)\right\}\delta_{r_4r_2}}{(q_1+p_5)^2-\mu^2} \qquad (48)$$

$$\begin{aligned}
\mathcal{M}_{4+5} &= -i2\frac{\mu^2}{f^2}\left(c_1^* + \frac{{p_5}^0{p_6}^0}{\mu^2}c_2^*\right)\left\{\frac{f_{\pi NN}}{\mu}\frac{\tilde{f}}{\mu}\left[\frac{(\vec{\sigma}\cdot\vec{q_2})_{r_3r_1}(\vec{\sigma}\cdot\vec{q_2})_{r_4r_2}}{\vec{q_2}^2}\left(V_L'(q_2)-V_T'(q_2)\right)\right.\right. \\
&\left.\left. +V_T'(q_2)(\vec{\sigma})_{r_3r_1}\cdot(\vec{\sigma})_{r_4r_2}\right] + g_{\sigma NN}g_{\sigma NN^*}\frac{\delta_{r_3r_1}\delta_{r_4r_2}}{q_2^2-m_\sigma^2}F_\sigma^2(q_2)\right\} \\
&\times\left[D_{N^*}(p_5+p_6+p_3)+D_{N^*}(p_5+p_6-p_1)\right] \qquad (49)
\end{aligned}$$

$$\mathcal{M}_{6+7} = 0 \qquad (\textit{not allowed by isospin symmetry}) \qquad (50)$$

$$\begin{aligned}
\mathcal{M}_8 &= i\frac{1}{9}\frac{f^*}{\mu}\frac{g_{\pi N^*\Delta}}{\mu}\left\{\frac{f_{\pi NN}}{\mu}\frac{\tilde{f}}{\mu}\left[\frac{(\vec{\sigma}\cdot\vec{q_2})_{mr_1}(\vec{\sigma}\cdot\vec{q_2})_{r_4r_2}}{\vec{q_2}^2}\left(V_L'(q_2)-V_T'(q_2)\right)\right.\right. \\
&\left.\left. +V_T'(q_2)(\vec{\sigma})_{mr_1}\cdot(\vec{\sigma})_{r_4r_2}\right] + g_{\sigma NN}g_{\sigma NN^*}\frac{\delta_{mr_1}\delta_{r_4r_2}}{q_2^2-m_\sigma^2}F_\sigma^2(q_2)\right\} \\
&\times\left\{2(\vec{p_5}\vec{p_6})\delta_{r_3m}\left[D_\Delta(p_5+p_3)+3D_\Delta(p_6+p_3)\right] - i(\vec{\sigma}\cdot[\vec{p_5}\times\vec{p_6}])_{r_3m}\right. \\
&\left.\times\left[D_\Delta(p_5+p_3)-3D_\Delta(p_6+p_3)\right]\right\}D_{N^*}(p_5+p_6+p_3) \qquad (51)
\end{aligned}$$

$$
\begin{aligned}
\mathcal{M}_9 &= i\left(\frac{f^*}{\mu}\right)^2 \frac{f_{\pi NN}}{\mu}\frac{f_\Delta}{\mu} D_\Delta(p_5+p_6+p_3) \\
&\times\Bigg[\frac{1}{9}\Bigg\{\frac{(\vec{\sigma}\cdot\vec{q_2})_{r_4r_2}}{\vec{q_2}^{\,2}}\left[5i(\vec{q_2}\cdot[\vec{p_5}\times\vec{p_6}])\delta_{r_3r_1}-(\vec{p_5}\cdot\vec{p_6})(\vec{\sigma}\cdot\vec{q_2})_{r_3r_1}\right. \\
&\quad \left.+4(\vec{p_5}\cdot\vec{q_2})(\vec{\sigma}\cdot\vec{p_6})_{r_3r_1}-(\vec{p_6}\cdot\vec{q_2})(\vec{\sigma}\cdot\vec{p_5})_{r_3r_1}\right](V_L'(q_2)-V_T'(q_2)) \\
&\quad +[5i\delta_{r_3r_1}(\vec{\sigma}\cdot[\vec{p_5}\times\vec{p_6}])_{r_4r_2}-(\vec{p_5}\cdot\vec{p_6})(\vec{\sigma})_{r_3r_1}\cdot(\vec{\sigma})_{r_4r_2} \\
&\quad +4(\vec{\sigma}\cdot\vec{p_6})_{r_3r_1}(\vec{\sigma}\cdot\vec{p_5})_{r_4r_2}-(\vec{\sigma}\cdot\vec{p_5})_{r_3r_1}(\vec{\sigma}\cdot\vec{p_6})_{r_4r_2}]\,V_T'(q_2)\Bigg\}D_\Delta(p_5+p_3) \\
&\quad -\frac{1}{6}\left\{\vec{p_5}\leftrightarrow\vec{p_6}\right\}D_\Delta(p_6+p_3)\Bigg] \qquad (52)
\end{aligned}
$$

$$
\begin{aligned}
\mathcal{M}_{10} &= i\frac{4\pi}{3}\left(\frac{f^*}{\mu}\right)^2\Bigg[\frac{1}{3}\frac{\left\{2\frac{\lambda_1}{\mu}+\frac{\lambda_2}{\mu^2}({q_2}^0+2{p_6}^0)\right\}\delta_{r_4r_2}}{(q_2+p_6)^2-\mu^2}\{2(\vec{p_5}\cdot(\vec{q_2}+\vec{p_6}))\delta_{r_3r_1} \\
&\qquad -i(\vec{\sigma}\cdot[\vec{p_5}\times(\vec{q_2}+\vec{p_6})])_{r_3r_1}\}D_\Delta(p_5+p_3) \\
&\qquad +\frac{\left\{2\frac{\lambda_1}{\mu}-\frac{\lambda_2}{\mu^2}({q_2}^0+2{p_5}^0)\right\}\delta_{r_4r_2}}{(q_2+p_5)^2-\mu^2}\{2(\vec{p_6}\cdot(\vec{q_2}+\vec{p_5}))\delta_{r_3r_1} \\
&\qquad -i(\vec{\sigma}\cdot[\vec{p_6}\times(\vec{q_2}+\vec{p_5})])_{r_3r_1}\}D_\Delta(p_6+p_3)\Bigg] \qquad (53)
\end{aligned}
$$

$$
\begin{aligned}
\mathcal{M}_{11} &= i\frac{4\pi}{3}\left(\frac{f^*}{\mu}\right)^2\Bigg[\frac{\left\{2\frac{\lambda_1}{\mu}+\frac{\lambda_2}{\mu^2}({q_2}^0+2{p_6}^0)\right\}\delta_{r_4r_2}}{(q_2+p_6)^2-\mu^2}\{2(\vec{p_5}\cdot(\vec{q_2}+\vec{p_6}))\delta_{r_3r_1} \\
&\qquad +i(\vec{\sigma}\cdot[\vec{p_5}\times(\vec{q_2}+\vec{p_6})])_{r_3r_1}\}D_\Delta(p_1-p_5) \\
&\qquad +\frac{1}{3}\frac{\left\{2\frac{\lambda_1}{\mu}-\frac{\lambda_2}{\mu^2}({q_2}^0+2{p_5}^0)\right\}\delta_{r_4r_2}}{(q_2+p_5)^2-\mu^2}\{2(\vec{p_6}\cdot(\vec{q_2}+\vec{p_5}))\delta_{r_3r_1} \\
&\qquad +i(\vec{\sigma}\cdot[\vec{p_6}\times(\vec{q_2}+\vec{p_5})])_{r_3r_1}\}D_\Delta(p_1-p_6)\Bigg] \qquad (54)
\end{aligned}
$$

$$
\begin{aligned}
\mathcal{M}_{12} &= i\frac{1}{3}\frac{1}{9}\left(\frac{f^*}{\mu}\right)^4\left(\frac{1}{(\vec{q_2}+\vec{p_6})^2}\left\{2(\vec{p}_6\cdot(\vec{q}_2+\vec{p}_6))\delta_{r_4r_2}-i(\vec{\sigma}\cdot[\vec{p_6}\times(\vec{q_2}+\vec{p_6})])_{r_4r_2}\right\}\right.\\
&\times\left\{2(\vec{p}_5\cdot(\vec{q}_2+\vec{p}_6))\delta_{r_3r_1}-i(\vec{\sigma}\cdot[\vec{p_5}\times(\vec{q_2}+\vec{p_6})])_{r_3r_1}\right\}(V_L'(q_2+p_6)-V_T'(q_2+p_6))\\
&+\left\{(\vec{p}_5\cdot\vec{p}_6)(-2\delta_{r_4r_1}\delta_{r_3r_2}+5\delta_{r_3r_1}\delta_{r_4r_2})+(\vec{\sigma}\cdot\vec{p}_5)_{r_4r_2}(\vec{\sigma}\cdot\vec{p}_6)_{r_3r_1}\right.\\
&\left.\left.+2i(\vec{\sigma}\cdot[\vec{p}_5\times\vec{p}_6])_{r_4r_2}\delta_{r_3r_1}-2i(\vec{\sigma}\cdot[\vec{p}_5\times\vec{p}_6])_{r_3r_1}\delta_{r_4r_2}\right\}V_T'(q_2+p_6)\right)\\
&\times D_\Delta(p_4+p_6)D_\Delta(p_3+p_5) \qquad (55)
\end{aligned}
$$

$$
\begin{aligned}
\mathcal{M}_{13} &= i\frac{1}{3}\frac{1}{9}\left(\frac{f^*}{\mu}\right)^4\left(\frac{1}{(\vec{q_2}+\vec{p_6})^2}\left\{2(\vec{p}_6\cdot(\vec{q}_2+\vec{p}_6))\delta_{r_4r_2}+i(\vec{\sigma}\cdot[\vec{p_6}\times(\vec{q_2}+\vec{p_6})])_{r_4r_2}\right\}\right.\\
&\times\left\{2(\vec{p}_5\cdot(\vec{q}_2+\vec{p}_6))\delta_{r_3r_1}+i(\vec{\sigma}\cdot[\vec{p_5}\times(\vec{q_2}+\vec{p_6})])_{r_3r_1}\right\}(V_L'(q_2+p_6)-V_T'(q_2+p_6))\\
&+\left\{(\vec{p}_5\cdot\vec{p}_6)(-2\delta_{r_4r_1}\delta_{r_3r_2}+5\delta_{r_3r_1}\delta_{r_4r_2})+(\vec{\sigma}\cdot\vec{p}_5)_{r_4r_2}(\vec{\sigma}\cdot\vec{p}_6)_{r_3r_1}\right.\\
&\left.\left.-2i(\vec{\sigma}\cdot[\vec{p}_5\times\vec{p}_6])_{r_4r_2}\delta_{r_3r_1}+2i(\vec{\sigma}\cdot[\vec{p}_5\times\vec{p}_6])_{r_3r_1}\delta_{r_4r_2}\right\}V_T'(q_2+p_6)\right)\\
&\times D_\Delta(p_2-p_6)D_\Delta(p_1-p_5) \qquad (56)
\end{aligned}
$$

$$
\begin{aligned}
\mathcal{M}_{14} &= i\frac{1}{9}\frac{1}{9}\left(\frac{f^*}{\mu}\right)^4\left(\frac{1}{(\vec{q_2}+\vec{p_6})^2}\left\{2(\vec{p}_6\cdot(\vec{q}_2+\vec{p}_6))\delta_{r_4r_2}+i(\vec{\sigma}\cdot[\vec{p_6}\times(\vec{q_2}+\vec{p_6})])_{r_4r_2}\right\}\right.\\
&\times\left\{2(\vec{p}_5\cdot(\vec{q}_2+\vec{p}_6))\delta_{r_3r_1}-i(\vec{\sigma}\cdot[\vec{p_5}\times(\vec{q_2}+\vec{p_6})])_{r_3r_1}\right\}(V_L'(q_2+p_6)-V_T'(q_2+p_6))\\
&+\left\{(\vec{p}_5\cdot\vec{p}_6)(2\delta_{r_4r_1}\delta_{r_3r_2}+3\delta_{r_3r_1}\delta_{r_4r_2})-(\vec{\sigma}\cdot\vec{p}_5)_{r_4r_2}(\vec{\sigma}\cdot\vec{p}_6)_{r_3r_1}\right.\\
&\left.\left.-2i(\vec{\sigma}\cdot[\vec{p}_5\times\vec{p}_6])_{r_4r_2}\delta_{r_3r_1}-2i(\vec{\sigma}\cdot[\vec{p}_5\times\vec{p}_6])_{r_3r_1}\delta_{r_4r_2}\right\}V_T'(q_2+p_6)\right)\\
&\times D_\Delta(p_2-p_6)D_\Delta(p_3+p_5) \qquad (57)
\end{aligned}
$$

$$
\begin{aligned}
\mathcal{M}_{15} &= i\frac{1}{9}\left(\frac{f^*}{\mu}\right)^4\left(\frac{1}{(\vec{q_2}+\vec{p_6})^2}\left\{2(\vec{p}_6\cdot(\vec{q}_2+\vec{p}_6))\delta_{r_4r_2}-i(\vec{\sigma}\cdot[\vec{p_6}\times(\vec{q_2}+\vec{p_6})])_{r_4r_2}\right\}\right.\\
&\times\left\{2(\vec{p}_5\cdot(\vec{q}_2+\vec{p}_6))\delta_{r_3r_1}+i(\vec{\sigma}\cdot[\vec{p_5}\times(\vec{q_2}+\vec{p_6})])_{r_3r_1}\right\}(V_L'(q_2+p_6)-V_T'(q_2+p_6))\\
&+\left\{(\vec{p}_5\cdot\vec{p}_6)(2\delta_{r_4r_1}\delta_{r_3r_2}+3\delta_{r_3r_1}\delta_{r_4r_2})-(\vec{\sigma}\cdot\vec{p}_5)_{r_4r_2}(\vec{\sigma}\cdot\vec{p}_6)_{r_3r_1}\right.\\
&\left.\left.+2i(\vec{\sigma}\cdot[\vec{p}_5\times\vec{p}_6])_{r_4r_2}\delta_{r_3r_1}+2i(\vec{\sigma}\cdot[\vec{p}_5\times\vec{p}_6])_{r_3r_1}\delta_{r_4r_2}\right\}V_T'(q_2+p_6)\right)\\
&\times D_\Delta(p_4+p_6)D_\Delta(p_1-p_5) \qquad (58)
\end{aligned}
$$

In these expressions p_1, p_2 ($p=(p^0,\vec{p})$) are the momenta of the incoming nucleons while p_3, p_4 are the momenta of the outgoing ones, p_5, p_6 are π^- and π^+ momenta respectively and $q_{1(2)}$ denote $p_{3(4)}-p_{1(2)}$. Here $r_3, r_4, r_1, r_2, m=(1,2)$ are spin indices and a sum in m is understood in Eq. (51) V_L' and V_T' are the longitudinal and transverse parts of the NN interaction as defined in Eq. (22), $F_\pi(q)$ and $F_\sigma(q)$ are pion and sigma form factors respectively. Finally $D_{N^*}(p)$ and $D_{\Delta^*}(p)$ stand for N^* and Δ propagators, given by the following expressions

$$
D_i(p)=\frac{1}{\sqrt{p^2}-M_i+\frac{1}{2}i\Gamma_i(p)}\frac{M_i}{\sqrt{M_i^2+\vec{p}_i^2}} \quad ; \qquad i=(N^*,\Delta). \qquad (59)
$$

Here $\Gamma_i(p)$ denotes the width of the resonance [11].

Figure Captions

Fig. 1. Complete set of Feynman diagrams of our model.

Fig. 2. Dominant mechanisms in the analysis of (α, α') performed in Ref. [11]. (a) Δ excitation in the projectile, (b) Roper excitation in the target.

Fig. 3. Total cross section for the $pp \to pp\pi^+\pi^-$ channel as a function of the incoming proton kinetic energy in the laboratory frame. Solid line, total (line labelled 1 for set I and 2 for set II of c_1^*, c_2^* parameters) ; long-short dashed line, $N^* \to N(\pi\pi)^{T=0}_{S-wave}$; long-dashed line, $N^* \to \Delta\pi$; dash-dotted line, Δ excitation mechanisms; short-dashed line, non-resonant terms from diagrams (1)-(3). The partial contributions are calculated with set I. Experimental data are taken from Refs. [12, 13, 14].

Fig. 4. $N^* \to N(\pi\pi)^{T=0}_{S-wave}$ contribution to $pp \to pp\pi^+\pi^-$ total cross section (set I) separated in $T = 0$ "σ" exchange (long-dashed line) and $T = 1$ correlated $\pi + \rho$ exchange (short-dashed line) pieces. The solid line gives their sum.

Fig. 5. Same as Fig. 3 for $pn \to pn\pi^+\pi^-$

Fig. 6. Same as Fig. 3 for $pp \to pn\pi^+\pi^0$

Fig. 7. Same as Fig. 3 for $pn \to pp\pi^-\pi^0$

Fig. 8. Same as Fig. 3 for $pp \to nn\pi^+\pi^+$

Fig. 9. Same as Fig. 3 for $pp \to pp\pi^0\pi^0$

Fig. 10. Same as Fig. 3 for $pn \to pn\pi^0\pi^0$

Fig. 11. Dominant mechanism in the $pp \to pp\pi^+\pi^-$ reaction at low energies with final state interaction included.

Fig. 12. Total cross section for the $pp \to pp\pi^+\pi^-$ channel with (dotted lines) and without (solid lines) final state interaction for both sets I and II.

References

[1] S. Weinberg, Phys. Rev. Lett. 18 (1967) 188; M.G. Olsson and L. Turner, Phys. Rev. Lett. 20 (1968) 1127.

[2] E. Oset and M.J. Vicente Vacas, Nucl. Phys. A446 (1985) 584.

[3] V. Bernard, N. Kaiser, U.G. Meissner, Nucl. Phys. B457 (1995) 147.

[4] M. Benmerrouche and E. Tomusiak, Phys. Rev. Lett 73 (1994)400.

[5] V. Bernard, N. Kaiser, U.G. Meissner and A. Schmidt, Nucl. Phys. A580 (1994) 475.

[6] J.A. Gómez Tejedor and E. Oset, Nucl. Phys. A571 (1994) 667.

[7] D. M Manley and E. M. Saleski, Phys. Rev. D45 (1992) 4002.

[8] J. A. Gómez Tejedor, F. Cano and E. Oset, Phys. Lett. B379 (1996) 39.

[9] J. A. Gómez Tejedor and E. Oset, Nucl. Phys. A600 (1996) 413.

[10] H. P. Morsch et al., Phys. Rev. Lett. 69 (1992) 1336.

[11] S. Hirenzaki, P. Fernández de Córdoba and E. Oset, Phys. Rev. C53 (1996) 277.

[12] D. C. Brunt, M. J. Clayton and B. A. Westwood, Phys. Rev. 187 (1969) 1856.

[13] F. Shimizu *et al.*, Nucl. Phys. A386 (1982) 571.

[14] L. G. Dakhno *et al.*, Sov. J. Nucl. Phys. 37 (1983) 540.

[15] K. Gasser and H. Leutwyler, Nucl. Phys. B250 (1985) 465.

[16] U. G. Meissner, Rep. Prog. Phys. 56 (1993) 903; V. Bernard, N. Kaiser and U. G. Meissner, Int. J. Mod. Phys. E4 (1995) 193.

[17] U. G. Meissner, E. Oset and A. Pich, Phys. Lett. B353 (1995) 161.

[18] F. Mandl and G. Shaw, Quantum Field Theory, Wiley-Interscience, 1984

[19] E. Oset and W. Weise, Nucl. Phys. A319 (1979) 365.

[20] R. Machleidt, K. Holinde and Ch. Elster, Phys. Rep. 149 (1987) 1.

[21] R. M. Barnett et al., Phys. Rev. D54 (1996) 1.

[22] E. Oset et al., Proc. of the CEBAF-INT Workshop on N^* resonances, Seattle 1996.

[23] T. S. Jensen and A. F. Miranda, Phys. Rev. C55 (1997) 1039.

[24] J. Prades, Z. Phys. C63 (1994) 491.

[25] I. Bar-Nir, T. Risser, M. D. Shuster, Nucl. Phys. B87 (1975) 109.

[26] F. Plouin, P. Fleury and C. Wilkin, Phys. Rev. Lett. 65 (1990) 690.

[27] E. Ferrari, Nuovo Cimento 30 (1963) 240.

[28] R. D. Amado, Modern three hadron physics, ed. A. W. Thomas (Springer, Berlin 1997).

[29] M. G. Olsson, Nucl. Phys. B78 (1974) 55.

[30] R. C. Carrasco and E. Oset, Nucl. Phys. A536 (1992) 445.

[31] M. Lacombe et al., Phys. Lett. B101 (1981) 139.

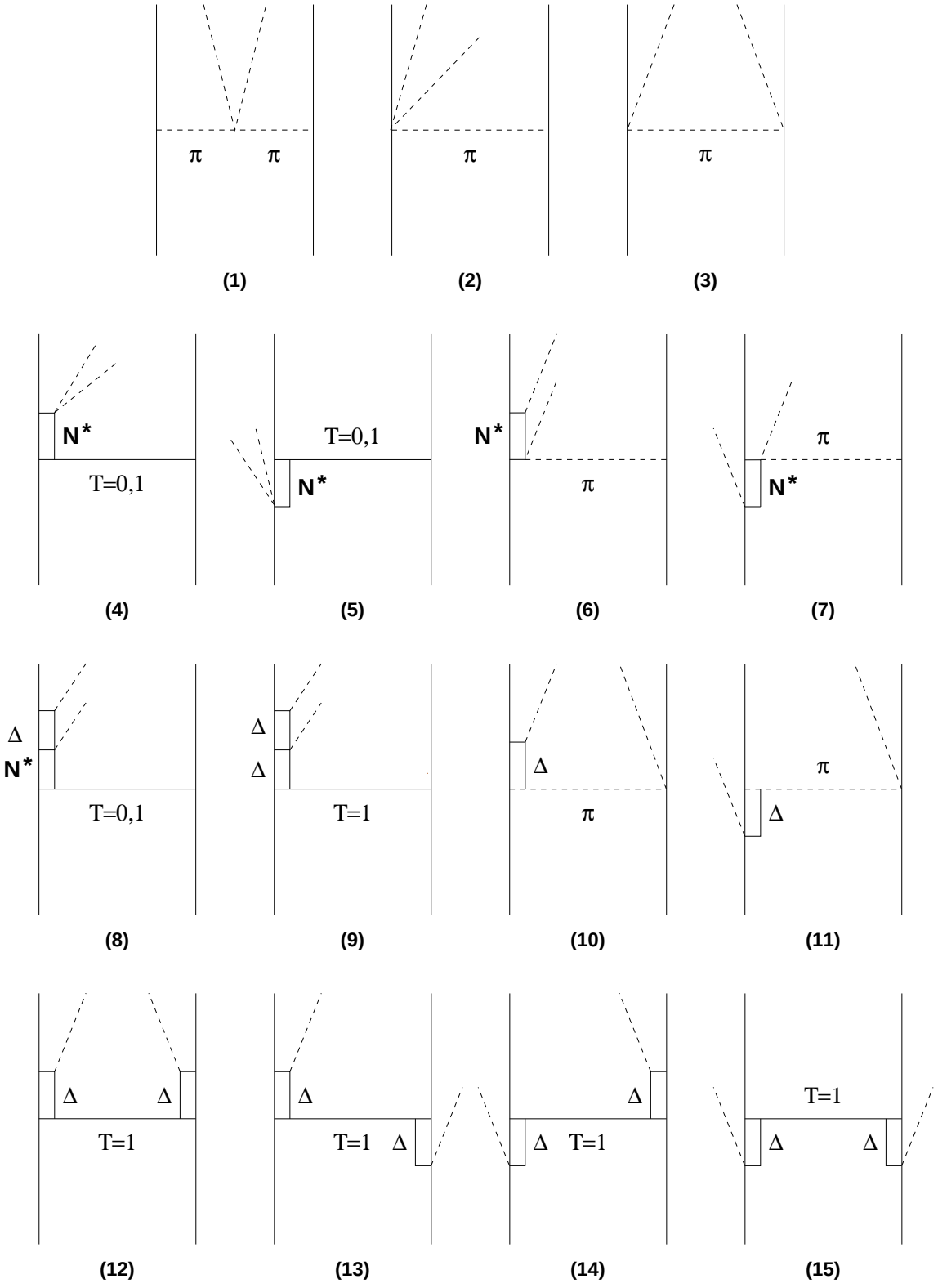
π
π
(1)
π
(2)
π
(3)
N*
T=0,1
(4)
T=0,1
N*
(5)
N*
π
(6)
π
N*
(7)
Δ
N*
T=0,1
(8)
Δ
Δ
T=1
(9)
Δ
π
(10)
π
Δ
(11)
Δ
Δ
T=1
(12)
Δ
T=1
Δ
(13)
Δ
Δ
T=1
(14)
T=1
Δ
Δ
(15)

Fig. 1

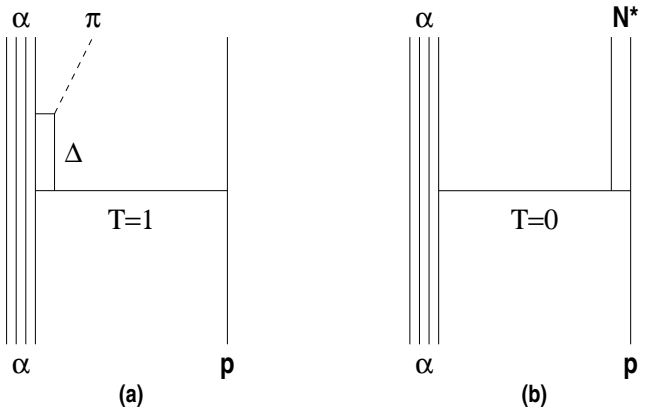

Fig 2

Fig. 3

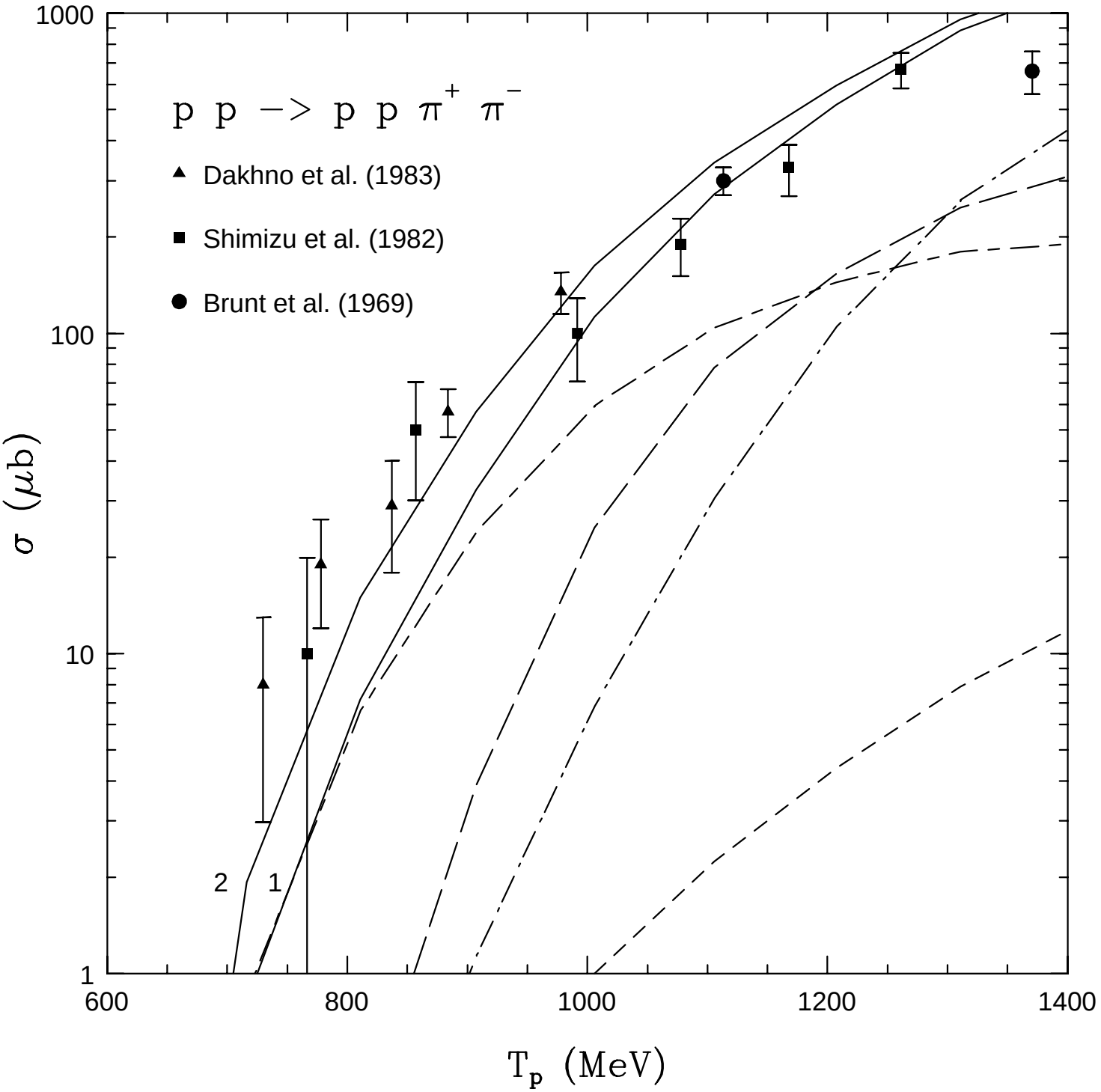
p p -> p p π+ π−
Dakhno et al. (1983)
Shimizu et al. (1982)
Brunt et al. (1969)
1000
100
10
1
σ (μb)
600
800
1000
1200
1400
T_p (MeV)
2
1

Fig. 4

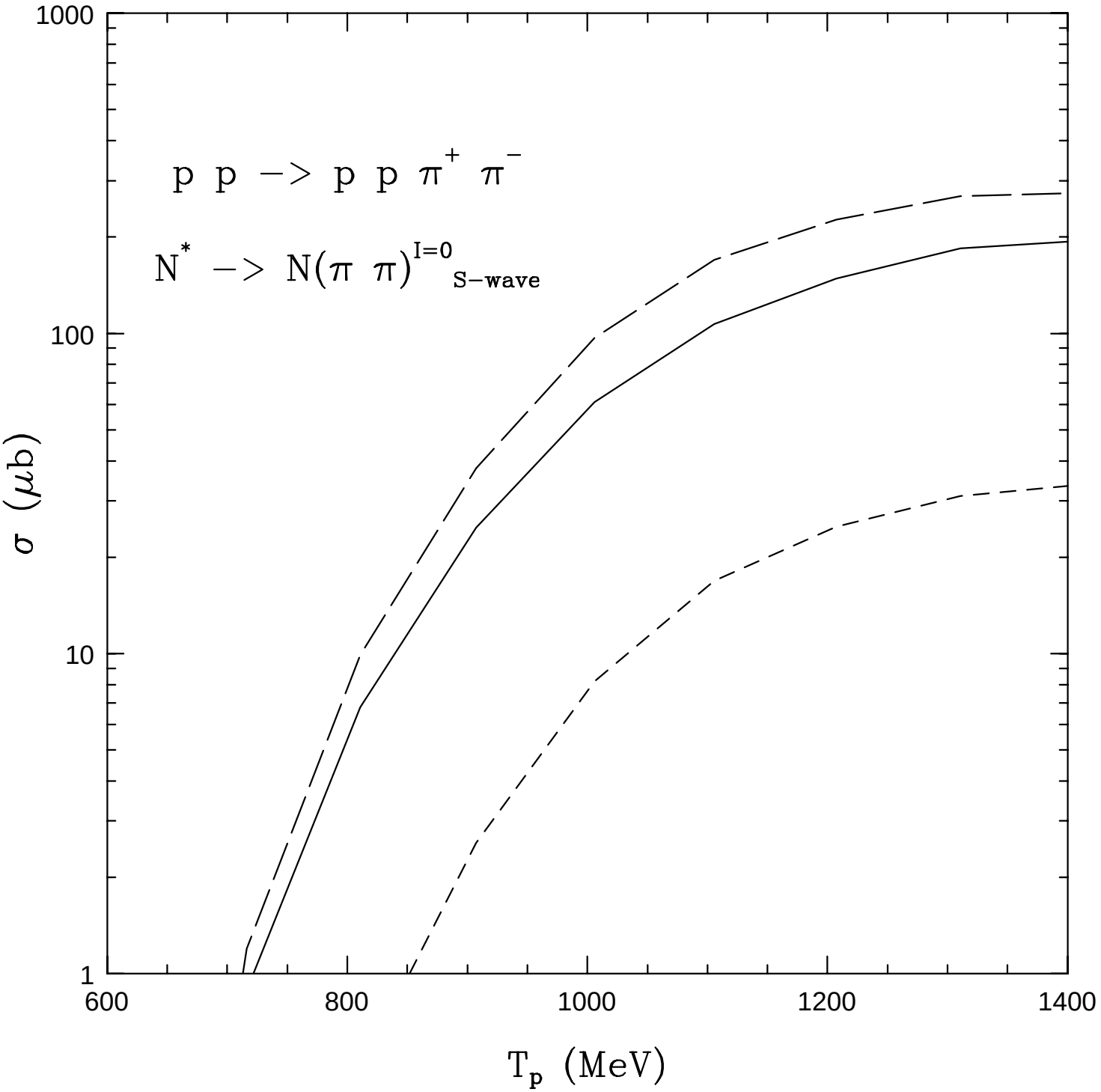
1000
100
10
1
600
800
1000
1200
1400
σ (μb)
T_p (MeV)
p p -> p p π+ π-
N* -> N(π π)I=0 S-wave

Fig. 5

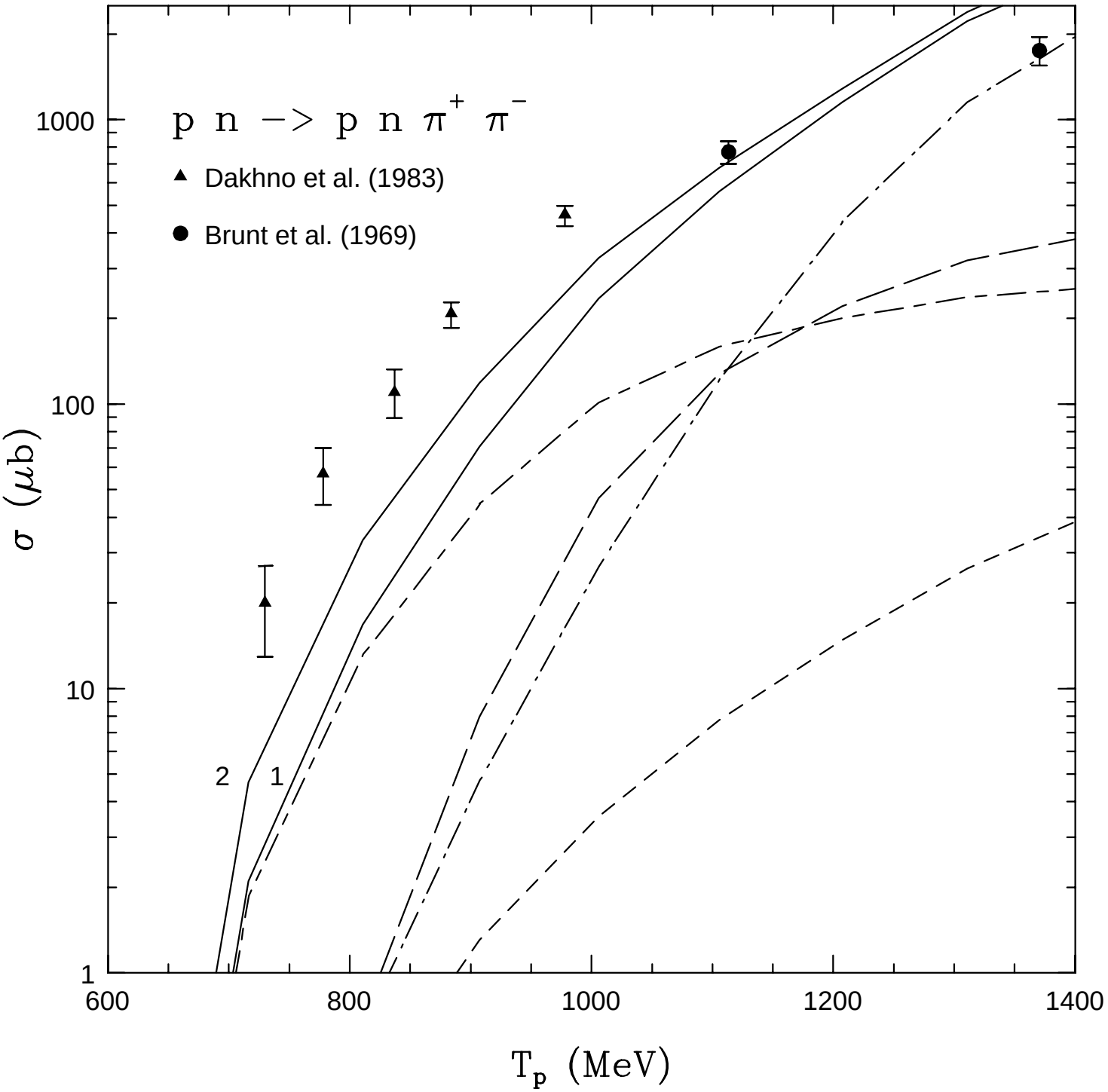
p n -> p n π+ π-
Dakhno et al. (1983)
Brunt et al. (1969)
σ (μb)
1000
100
10
1
600
800
1000
1200
1400
T_p (MeV)
2
1

Fig. 6

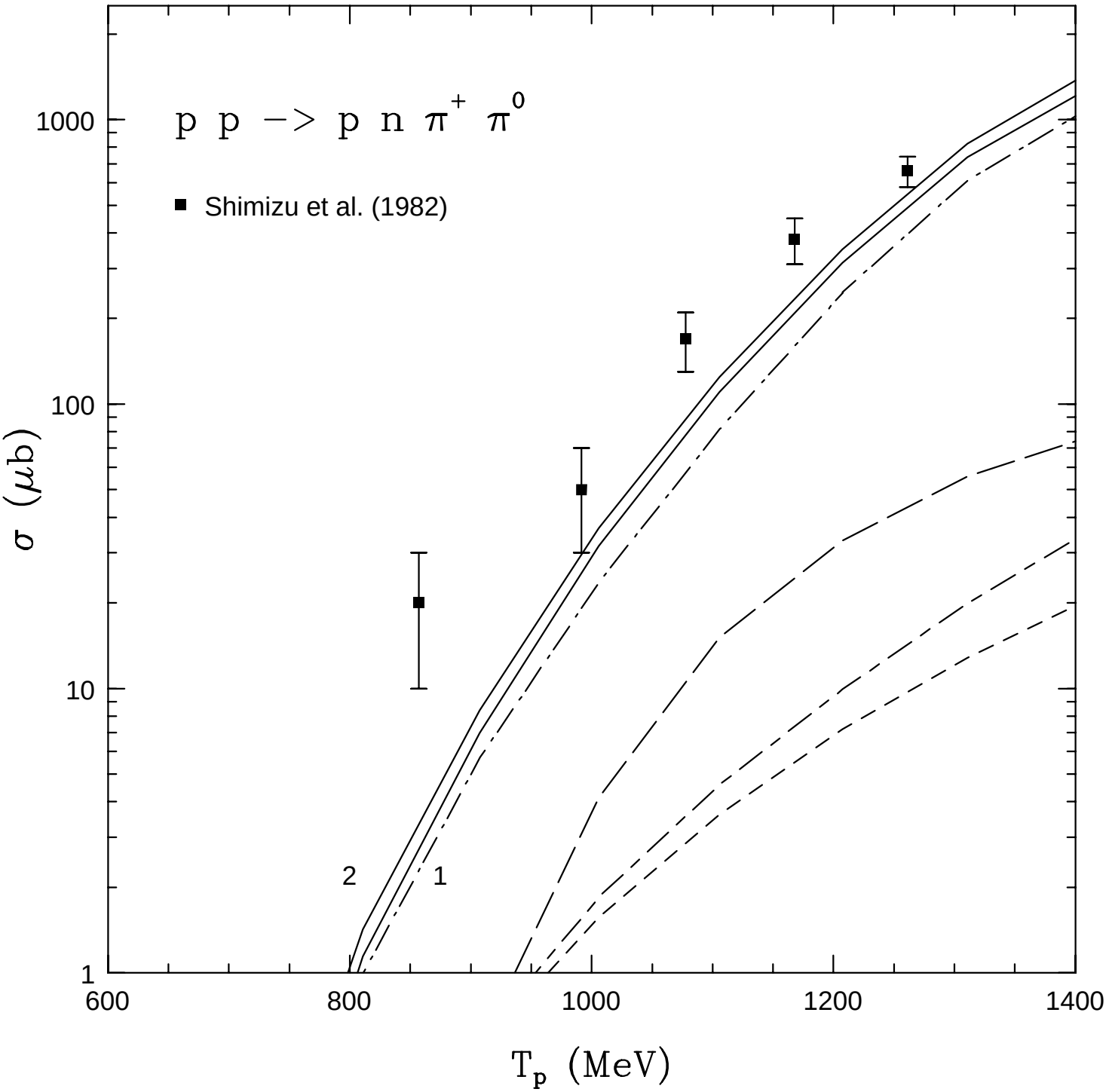
p p -> p n π+ π0
Shimizu et al. (1982)
1000
100
10
1
σ (μb)
600
800
1000
1200
1400
Tp (MeV)
2
1

Fig. 7

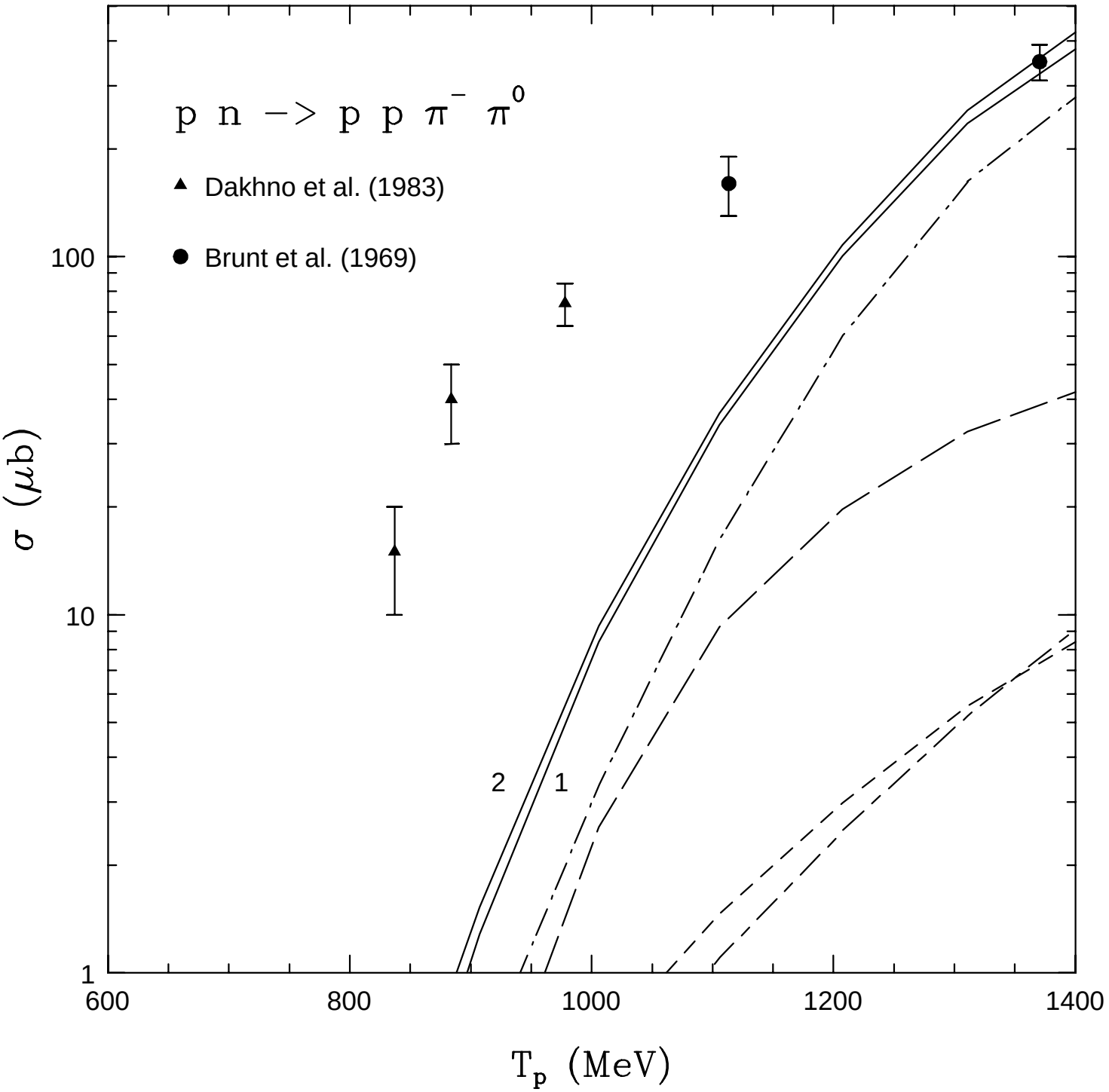
p n -> p p π⁻ π⁰
Dakhno et al. (1983)
Brunt et al. (1969)
100
10
1
σ (μb)
600
800
1000
1200
1400
T_p (MeV)
2
1

Fig. 8

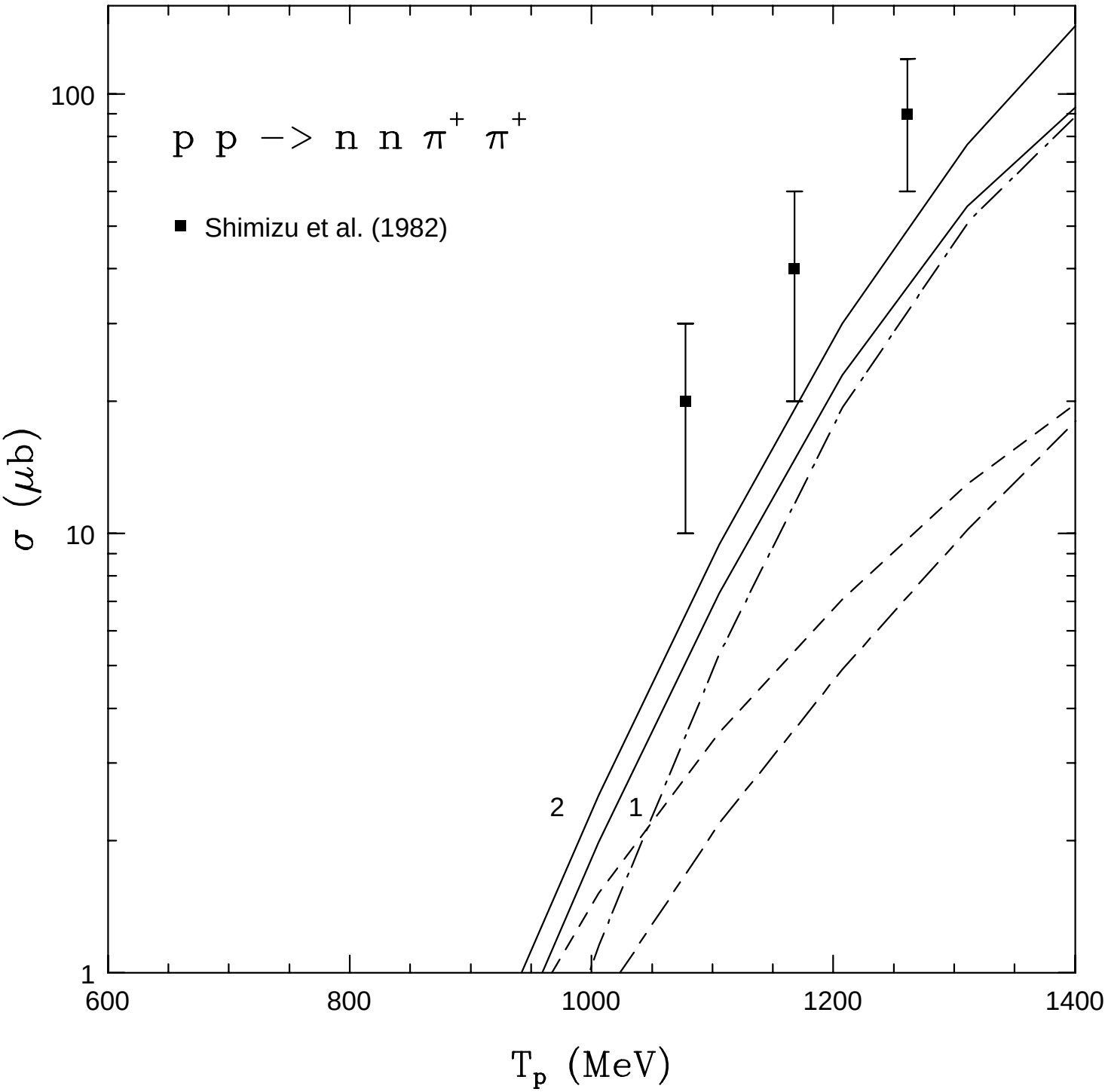
p p -> n n π+ π+
Shimizu et al. (1982)
100
10
1
σ (μb)
600
800
1000
1200
1400
T_p (MeV)
2
1

Fig. 9

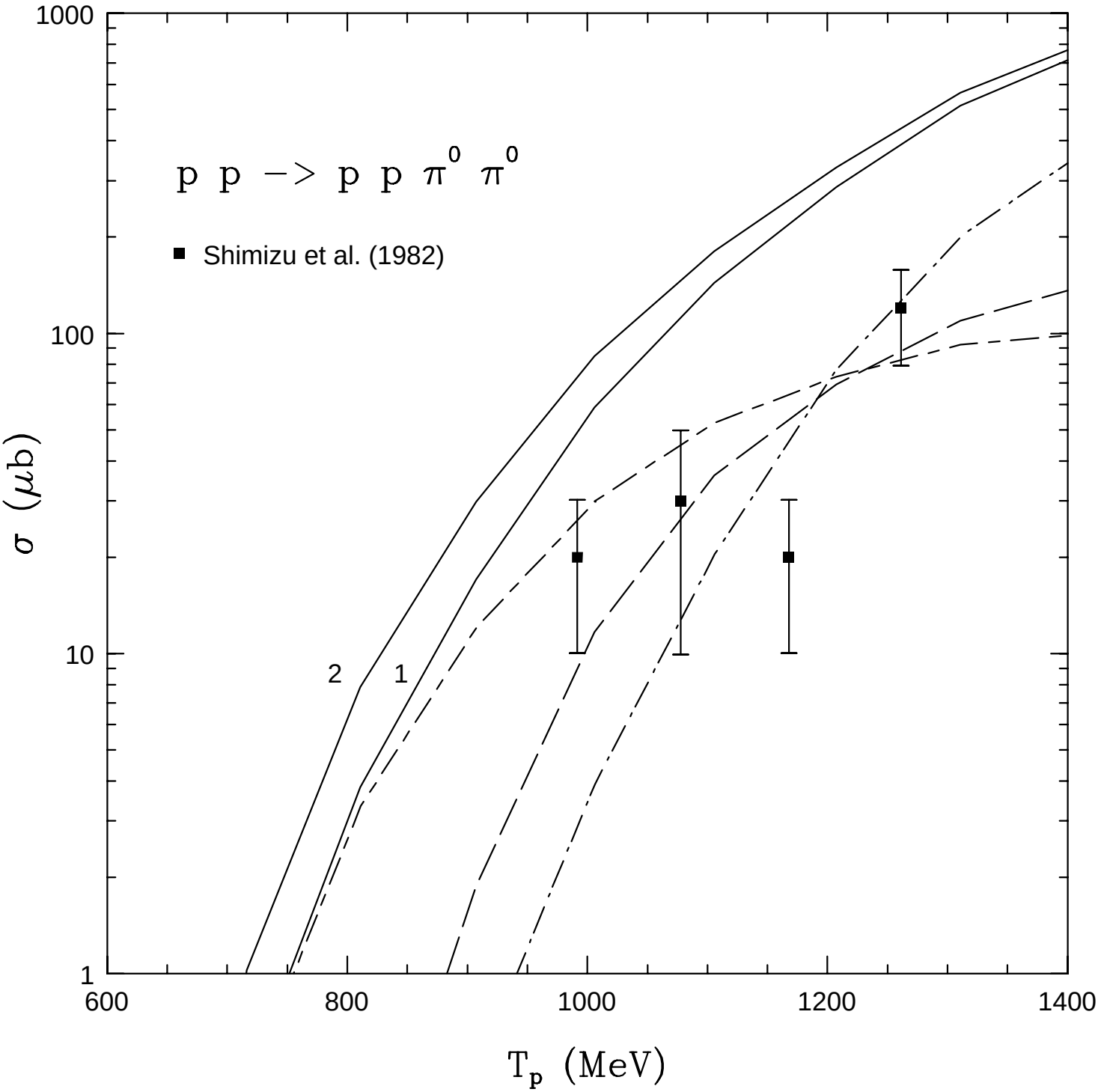
1000
100
10
1
600
800
1000
1200
1400
p p -> p p π⁰ π⁰
Shimizu et al. (1982)
2
1
σ (μb)
T_p (MeV)

Fig. 10

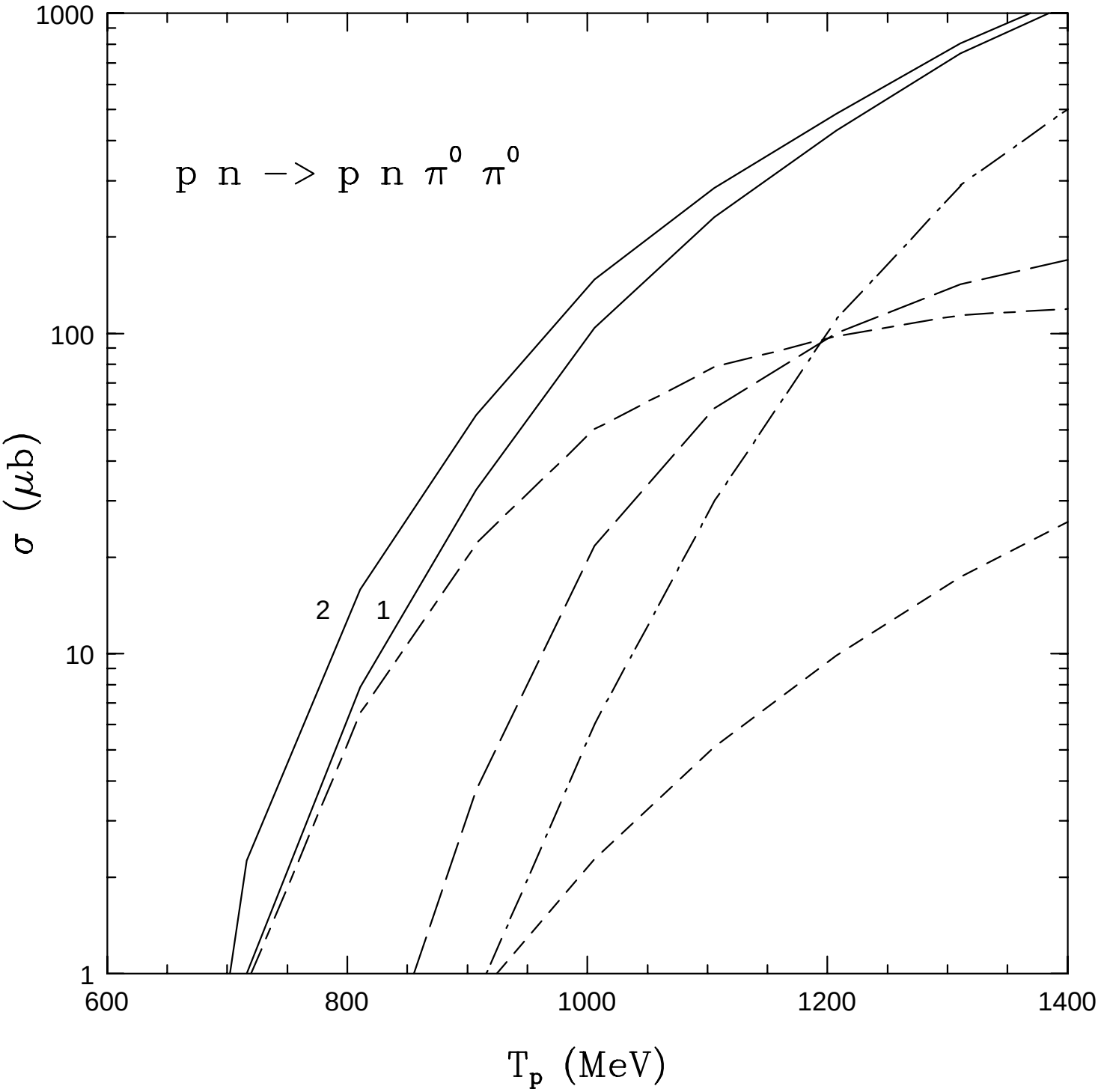

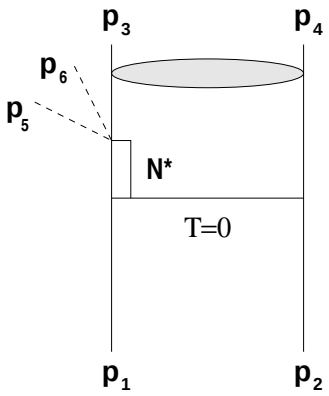

Fig 11

Fig. 12

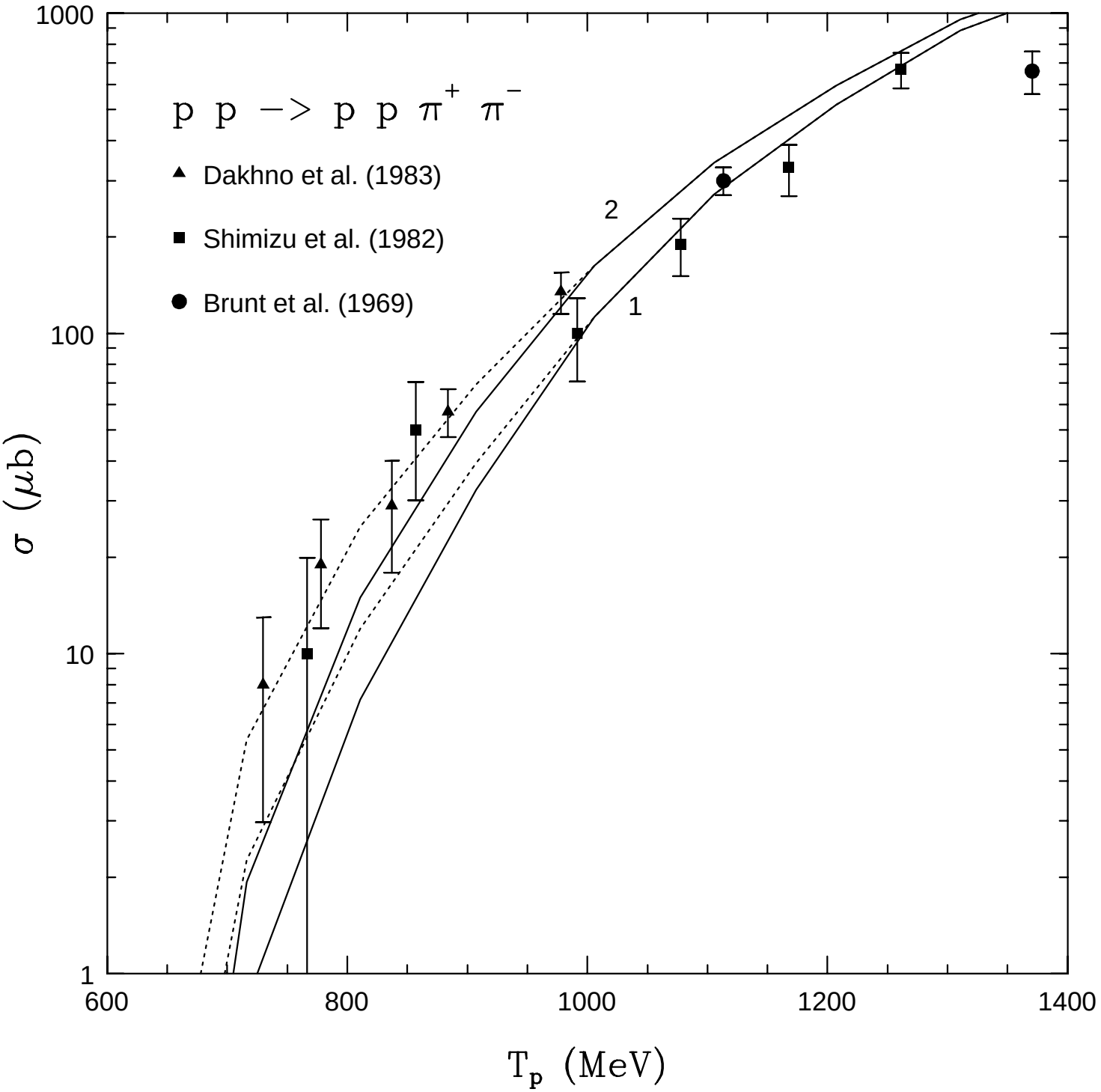
p p -> p p π+ π−
Dakhno et al. (1983)
Shimizu et al. (1982)
Brunt et al. (1969)
1
2
1000
100
10
1
σ (μb)
600
800
1000
1200
1400
Tp (MeV)